Hydrol. Earth Syst. Sci. Discuss., 12, 7267–7325, 2015
www.hydrol-earth-syst-sci-discuss.net/12/7267/2015/
doi:10.5194/hessd-12-7267-2015

Hydrology and Earth System Sciences
Discussions
Open Access

High-end climate change impact on European water availability and stress: exploring the presence of biases

L. V. Papadimitriou[1], **A. G. Koutroulis**[1], **M. G. Grillakis**[1], **and I. K. Tsanis**[1,2]

[1]Technical University of Crete, School of Environmental Engineering, Chania, Greece
[2]McMaster University, Department of Civil Engineering, Hamilton, ON, Canada

Received: 27 May 2015 – Accepted: 4 July 2015 – Published: 31 July 2015

Correspondence to: I. K. Tsanis (tsanis@hydromech.gr)

Published by Copernicus Publications on behalf of the European Geosciences Union.

Abstract

Climate models project a much more substantial warming than the 2 °C target making higher end scenarios increasingly plausible. Freshwater availability under such conditions is a key issue of concern. In this study, an ensemble of Euro-CORDEX projections under RCP8.5 is used to assess the mean and low hydrological states under +4 °C of global warming for the European region. Five major European catchments were analyzed in terms of future drought climatology and the impact of +2 vs. +4 °C global warming was investigated. The effect of bias correction of the climate model outputs and the observations used for this adjustment was also quantified. Projections indicate an intensification of the water cycle at higher levels of warming. Even for areas where the average state may not considerably be affected, low flows are expected to reduce leading to changes in the number of dry days and thus drought climatology. The identified increasing or decreasing runoff trends are substantially intensified when moving from the +2 to the +4 °C of global warming. Bias correction resulted in an improved representation of the historical hydrology. It is also found that the selection of the observational dataset for the application of the bias correction has an impact on the projected signal that could be of the same order of magnitude to the selection of the RCM.

1 Introduction

Global CO_2 emission rates keep following high-end climate change pathways leading to a future global temperature that is likely to surpass the target limit of 2 °C, despite the recent hiatus (England et al., 2015), and reach levels of +4 °C and higher at the end of the 21st century. By that time, the seasonality of river discharge is expected to get more pronounced for one-third of the global land surface, which translates to increased high flows and decreased low flows (Van Vliet et al., 2013). By the mid-century, the hydrological regime is projected to change considerably for a significant part of the

HESSD
12, 7267–7325, 2015

global land surface (Arnell and Gosling, 2013). The effect that global warming can have on water resources raises serious concerns on future water availability, especially under the pressure of the growing global population and the consequent increased food production needs. It is projected that the number of people coping with significantly reduced water availability will increase by 15 % globally due to climate change, while increased is also projected to be the percentage of the global population living under conditions of absolute water scarcity (Schewe et al., 2014).

In this framework, the future hydrological state needs to be assessed, in terms of both freshwater availability and water stresses. The runoff production is the component of the hydrological cycle most representative to describe these aspects, as it expresses the amount of available water after the evapotranspiration and infiltration losses and before any stream formation process intervenes. Furthermore, ensembles of mean annual and seasonal runoff can provide information about the climate change impact on river flows (Döll and Schmied, 2012). Studies have shown that changes in runoff are not linearly correlated with changes in global mean temperature (Arnell and Gosling, 2013), neither are meteorological with hydrological droughts (van Huijgevoort et al., 2013), concluding that for climate change impact assessments is fundamental to use an impact model to translate the precipitation derived signal into runoff.

A substantial number of large scale climate change impact studies that have been performed recently examine the future hydrological state analyzing projections of runoff or river flow. Fung et al. (2011) compared the projected future water availability under +2 and +4 °C of global warming, forcing the MacPDM Global Hydrological Model (GHM) with 22 GCMs from the CMIP3 experiment. Arnell and Gosling (2013) performed a global assessment of the climate driven changes in runoff based hydrologic indicators in mid-21st century, using multiple scenarios derived from the CMIP3 experiment. Schneider et al. (2013) focused on the impacts of climate change for the European river flows, using data from three bias corrected GCM scenarios. Van Vliet et al. (2013) performed a global assessment of future river discharge and temperature under two climate change scenarios, forcing a GHM with an ensemble of

HESSD
12, 7267–7325, 2015

bias corrected GCM output. They found that the combination of lower low flows with increased river water temperature can lead to water quality and ecosystem degradation in south-eastern United States, Europe, eastern China, southern Africa and southern Australia. An investigation of the future trends in flood risk at the global scale was performed by Dankers et al. (2014) and for the European region by Alfieri et al. (2015). The results of the latter study indicate that future flood hazard is mostly affected by the increased frequency of discharge extremes, rather than the absolute increase of discharge values. Betts et al. (2015) performed a global assessment of the impact posed on river flows and terrestrial ecosystems by climate and land use changes described by four RCPs. The study showed that, for all the climate scenarios, global warming in conjunction with elevated CO_2 concentrations result in augmented river outflows by the end of the 21st century.

Other studies assess climate change impacts under the adding stresses of population growth and human activities. Hanasaki et al. (2013) used different combinations of socio-economic and emission scenarios to capture the effects of a wide range of climate change scenarios on future water availability. Future climate was described by 3 GCMS and the water cycle was simulated in conjunction with water demand. Their results report increased water scarcity by the end of the 21st century, even for the lower-end emission and water use changes scenario, mainly due to the increasing population in developing countries and to general changes posed by global warming on the hydrological regime. Arnell and Lloyd-Hughes (2014) examined the effects of different degrees of climate change and future population scenarios on global water resources, using a large ensemble of 19 CMIP5 climate models. Their study underlined the importance of quantifying and accounting for the adaptation and mitigation challenges when assessing climate change impacts. Haddeland et al. (2014) investigated the impact of climate change and human interventions on global water resources. According to the study findings, the stress posed by human activities is similar, and in some cases more intense, than a respective stress caused by a +2 °C global warming scenario. Hejazi et al. (2014) analysed the cross-sectorial changes

HESSD
12, 7267–7325, 2015

Title Page
Abstract Introduction
Conclusions References
Tables Figures
◀| |▶
◀ ▶
Back Close
Full Screen / Esc
Printer-friendly Version
Interactive Discussion

of water needs under climate change. Results indicate that while water scarcity is an issue that many regions (mainly Middle East and India) will have to tackle with, for other regions (e.g. USA and Canada) climate change is likely to alleviate water shortage problems.

Multi-model assessments have been performed in an attempt to quantify the climate change analysis' uncertainty resulting from the impact model. Hagemann et al. (2013), performed future hydrological simulations with 3 GCMs and 8 GHMs. According to their findings, impact model induced uncertainty is larger than that of the GCMs for some regions of the land surface. With a global multi-model experiment van Huijgevoort et al. (2013) investigated the impact models' agreement on the effect of global warming on global drought in runoff and concluded that there are significant differences in the simulated drought event duration and spatial extent between the models. Comparing simulations from 9 GHMs and LSMs, Dankers et al. (2014) found that the impact models and the driving GCMs exhibit consistency in the projected patterns of flood risk at the large-scale, but significant disagreements are found at the local scale, which may regard even the sign of the change. This increased basin scale uncertainty is an important issue to cope with when studying climate change adaptation locally (Dankers et al., 2013).

Currently, global mean temperature has increased 0.85 °C relative to pre-industrial and already 18 % of the moderate daily precipitation extremes is attributed to this warming. At +2 °C the fraction of the global warming driven precipitation extremes is projected to rise up to 40 % (Fischer and Knutti, 2015). The effect of a 2 °C global warming for the European climate was examined by Vautard et al. (2014). The study revealed that warming in Europe is projected to be higher than the global average of 2 °C. Prospects of limiting the warming to this target have become vanishingly small (Sanford et al., 2014) at the same time that many experts believe that we are on the +4 °C path (Betts et al., 2011, 2015).

Significant climate change induced alterations are projected for the flow regime in Europe, with the most pronounced changes in magnitude projected for the

HESSD
12, 7267–7325, 2015

Mediterranean region and the northern part of the continent (Schneider et al., 2013). Moreover, considering that southern Europe is identified as a possible hotspot where the fraction of land under drought will increase substantially (Prudhomme et al., 2014), along with global temperature rise exceeding +2 °C, concerns for future water availability in Europe are raising. Prolonged water deficits during long-term droughts surpass the resilience of the hydrological systems and are a significant threat to water resources security in Europe (Parry et al., 2012). In the Euro-Mediterranean regions the severity of droughts has increased during the past 50 years, as a consequence of greater atmospheric evaporative demand resulting from temperature rise (Vicente-Serrano et al., 2014). Besides southern European areas, north-western and central-eastern regions appear more drought prone than the rest of Europe (Bonaccorso et al., 2013). Streamflow projections indicate more severe and persistent droughts in many parts of Europe due to climate change, except for northern and north-eastern parts of the continent. The opposite is projected for the middle and northern parts with a highly significant signal of reduced droughts that may be reversed due to intensive water use (Forzieri et al., 2014). Consequently European cropland affected by droughts is projected to increase 7-fold (up to 700 000 $km^2 year^{-1}$) at about +3 °C of global warming (Ciscar et al., 2014) compared to the situation of the last decades. Similarly, under the same warming level, European population affected by droughts is expected to increase by a factor of seven, overcoming the 150 million $year^{-1}$.

GCM outputs, used as input in impact models to assess the effects of climate change, feature systematic errors and biases. To deal with these, several bias correction techniques have been developed to statistically adjust the GCM output against observations. This process adds another level of uncertainty in the chain of climate to impact modelling that has to be investigated and communicated to the impact research communities. Ehret et al. (2012) acknowledge the fact that inherent climate models' biases render them unsuitable for direct use in climate change impact assessments but express scepticism towards adopting bias correction as a standard undisputed procedure. They argue that bias adjustment hides rather than reduces

HESSD
12, 7267–7325, 2015

the uncertainty, as the narrowing of the uncertainty range is not supported by any physical explanation. Teutschbein and Seibert (2012) also accept the need for bias correction but raise awareness towards the increased uncertainty derived from adding this step to the modelling chain. Ehret et al. (2012) introduce the issue of how "correct" is the dataset used as baseline for the bias adjustment. Haerter et al. (2011) underline that the statistical adjustments applied to GCM data with bias correction are bounded to the timescale selected for the adjustment and might have adverse effects on the statistics of another timescale. Haerter et al. (2011) also accentuate that one significant assumption is made when present day based bias correction methods are applied to climate scenario simulations; that of the bias stationarity throughout the future decades. Teng et al. (2015) argue that errors in bias corrected precipitation are inherited and augmented in modelled runoff.

Until climate modelling development manages to overcome the biases included in model outputs, GCM data are not an adequate forcing for GHMs. Bias correction is a helpful tool to deal with this problem, as its application improves the representation of both mean flow and seasonality and is thus fundamental for climate change analysis (Harding et al., 2014).

The major tools for the investigation of large scale hydrological changes due to climate change are Global Hydrological Models (GHMs) and/or Land Surface Models (LSMs). GHMs describe the lateral transfer of water and are focused on water resources (Haddeland et al., 2011) while LSMs focus on flux exchanges mainly at the vertical direction, simulating the energy, water and carbon exchanges between the land surface and the atmosphere (Zulkafli et al., 2013), as they were originally developed to provide the lower boundary for climate models. It should be noted however that for some models their classification in one of the two categories cannot be definitive, and they have been reported in the literature both as GHMs and as LSMs. According to the classification proposed by Haddeland et al. (2011), the models that solve the water balance are considered as GHMs and the models that solve both the water and energy balance are categorized as LSMs. Several references on Global Models and

HESSD
12, 7267–7325, 2015

their applications in water related modelling applications follow. WaterGAP (Alcamo et al., 2003) is a GHM well applicable for simulating the effects of climate change on water availability and irrigation demands (Döll et al., 2003; Verzano, 2009), which has been used to simulate inter-sectorial water uses under socio-economic development (Flörke et al., 2013) and to assess changes in flow regimes in Europe due to climate change (Schneider et al., 2013) and the resulting ecological risk for rivers (Laizé et al., 2013). The GHM MacPDM (Arnell, 1999) has been used in various recent studies to estimate climate change effects on global water scarcity (Gosling and Arnell, 2013) and global river flow regimes (Arnell and Gosling, 2013) and for assessing the effects of climate policy on the impacts of climate change (Arnell et al., 2013). The LSM H08 (Hanasaki et al., 2008) has been used in global applications for the estimation of river flows and sources of virtual water used for agriculture and livestock products (Hanasaki et al., 2010).

The LSM JULES (Joint UK Land Environment Simulator) has been implemented for many recent climate change impact and model inter- comparison studies (Hagemann et al., 2013; Davie et al., 2013; Dankers et al., 2014; Prudhomme et al., 2014; Harding et al., 2014). Furthermore, JULES has been used in many recent studies as a tool for evaluating the exchange of water, energy and carbon fluxes between the land surface and the atmosphere. Van den Hoof et al. (2013) assessed JULES' performance in simulating evaporative flux (and its partitions) and carbon flux in temperate Europe and evaluated an adapted version of the model for its suitability for use in climate change studies, based on the extreme summer of 2003. Marthews et al. (2012) implemented JULES in tropical forests of Andes-Amazon to simulate all components of carbon balance and study possible flux variations between sites of different altitude. Zulkafli et al. (2013) implemented JULES in a humid tropical mountain basin of the Peruvian Andes-Amazon. MacKellar et al. (2013) evaluated JULES, implemented in a region of Southern Africa, concerning its ability to simulate the catchment streamflow, testing both the PDM and the TOPMODEL runoff generation schemes. In the study of Bakopoulou et al. (2012), the sensitivity of the JULES outputs to the soil parameters of

HESSD
12, 7267–7325, 2015

the model at a point scale was estimated. Dadson et al. (2010) sought to quantify the feedback between wetland inundation and heat and moisture fluxes in the Niger inland delta by adding an overbank flow parameterization into JULES. Burke et al. (2013) used JULES to simulate retrospectively the pan-arctic changes in permafrost and Dankers et al. (2011) assessed JULES' performance in simulating the distribution of surface permafrost in large scale catchments. In a study by Jiménez et al. (2013) soil moisture modelled with JULES is evaluated against satellite soil moisture observations.

The scope of this work is to assess future water availability and identify water stress conditions in the European region under high-end scenarios of climate change. Transient hydrological simulations for the period 1971–2100 were performed by forcing the JULES model with five Euro-CORDEX (Coordinated Downscaling Experiment over Europe) climate projections. Water availability is described by the output of runoff production. In our analysis the model results are mainly interpreted statistically, aiming to express the changes found in the projected future periods with respect to the historical baseline state rather than describing future regimes with absolute numbers. The aspects that are examined here include:

1. Changes posed on the hydrological cycle (mean state and lower extremes) at +4 °C global warming compared to a baseline situation, and relative to the target of 2 °C warming.

2. The effect of bias correction on projected hydrological simulations. Both raw and bias corrected Euro-CORDEX data were used as input forcing in the impact model.

3. The effect of the observational dataset used for bias correction.

4. Drought climatology, along with climate change induced changes, at the basin scale.

HESSD
12, 7267–7325, 2015

2 Data and methods

Hydrological simulations were performed with the JULES Land Surface Model driven by Euro-CORDEX climate scenarios. To warm-up the model, 10 spin-up cycles from 1955 to 1960 were run. A daily time-step was employed for all the model runs. JULES was setup at the spatial resolution of the forcing Euro-CORDEX data which was 0.44°. The model output was regridded to match a 0.5° × 0.5° grid.

Brief descriptions of the climate data and the impact model are included in the following sections.

2.1 Climate data

Projections from five Euro-CORDEX experiments under Representative Concentration Pathway RCP8.5 scenario were used as input to JULES. The climate models were selected so as to cover the range of model sensitivity, as expressed by the index of Equilibrium climate sensitivity (ECS) which spans from 2.1 to 4.7 K for the CMIP5 ensemble (Andrews et al., 2012). ECS is a useful metric of the response of a climate model, in terms of air temperature change, to a doubling of the atmospheric CO_2 concentration (Andrews et al., 2012). Another factor for selecting the participating climate models was the availability of GCM downscaled at the spatial resolution of 0.44°.

Historical and projected time-slices comprise of 30 years of simulations, for which one time-slice average is extracted. The historical or baseline time-slice covers the period from 1976 to 2005. The projected time-slice varies between the models. The definition for determining the projected time-slice here is to take the 30 year average of the slice centered on the year where the +4 Specific Warming Level (SWL) is exceeded. The reference period for the calculation of the SWL is the pre-industrial state and specifically the period from 1861 to 1880. For three of the selected scenarios the +4 SWL is achieved outside the temporal extend of this study, thus the last 30 year period available is considered instead (2071–2100). The SWL exceeded during that

HESSD
12, 7267–7325, 2015

period for the models that reach +4 after 2100 is shown in Table 1. For reasons of consistency in terminology the time-slice of all models describing the greater SWL achieved will be referred to as +4 SWL time-slice.

The five scenarios along with information on the time-slices extracted for our analysis and the corresponding exceeded warming levels and ECS indices are shown in Table 1. Two widely used observational datasets were used to adjust the biases of the RCMs precipitation and temperature data. The first dataset was a hybrid dataset created by the Inter-Sectoral Impact Model Integration and Intercomparison Project ISI-MIP (Warszawski et al., 2014) that consists of the WFD (Weedon et al., 2010) and WFDEI-GPCC (Weedon et al., 2014) datasets. Additionally, the station data based European Climate Assessment and Dataset (ECA&D) and the ENSEMBLES Observations gridded dataset (E-OBS v10; Haylock et al., 2008) was also used for the bias adjustment of the aforementioned climate variables.

2.2 The JULES land surface model

JULES is a physically based land surface model that was established in 2006. It is comprised of two parts: the Met Office Surface Exchange Scheme (MOSES; Cox et al., 1998) and the Top-down Representation of Interactive Foliage and Flora Including Dynamics (TRIFFID; Cox, 2001) component. MOSES is an energy and water balance model which is JULES' forerunner, and TRIFFID is a dynamic global vegetation model (Best et al., 2011; Clark et al., 2011; Cox, 2001). In our model application for this study we do not examine vegetation dynamics thus we are focusing on the MOSES component of JULES.

The meteorological forcing data required for running JULES are: downward shortwave and longwave radiation, precipitation rate, air temperature, wind-speed, air pressure and specific humidity (Best et al., 2011).

JULES has a modular structure, which makes it a flexible modelling platform, as there is the potential of replacing modules or introducing new modules within the model. The physics modules that comprise JULES include the following themes: surface exchange

HESSD
12, 7267–7325, 2015

of energy fluxes, snow cover, surface hydrology, soil moisture and temperature, plant physiology, soil carbon and vegetation dynamics (Best et al., 2011), with the latter being disabled for this application.

In JULES, each gridbox is represented with a number of surface types, each one represented by a tile. JULES recognises nine surface types (Best et al., 2011), of which five are vegetation surface types (broadleaf trees, needleleaf trees, C3 (temperate) grasses, C4 (tropical) grasses and shrubs) and four are non-vegetated surface types (urban, inland water, bare soil and ice). A full energy balance equation including constituents of radiation, sensible heat, latent heat, canopy heat and ground surface heat fluxes is calculated separately for each tile and the average energy balance for the gridbox is found by weighting the values from each tile (Pryor et al., 2012).

In JULES the default soil configuration consists of four soil layers of thicknesses 0.1, 0.25, 0.65 and 2.0 m. This configuration however can be altered by the user. The fluxes of soil moisture between each soil layer are described by Darcy's law and a form of Richards' equation (Richards, 1931) governs the soil hydrology. Runoff production is governed by two processes: infiltration excess surface runoff and drainage through the bottom of the soil column, a process calculated as a Darcian flux assuming zero gradient of matric potential (Best et al., 2011). There is also the option of representing soil moisture heterogeneity. In that case total surface runoff also includes saturation excess runoff. The model allows for two approaches to introduce sub-grid scale heterogeneity into the soil moisture: (1) use of TOPMODEL (Beven and Kirkby, 1979), where heterogeneity is taken into account throughout the soil column, or (2) use of PDM (Moore, 1985), which represents heterogeneity in the top soil layer only (Best et al., 2011). Calculation of potential evaporation follows the Penman–Monteith approach (Penman, 1948). Water held at the plant canopy evaporates at the potential rate while restrictions of canopy resistance and soil moisture are applied for the simulation of evaporation from soil and plant transpiration from potential evaporation.

JULES simulates fluxes at the vertical direction only. For hydrological applications this means that the model calculates runoff production in each gridbox which needs to

HESSD
12, 7267–7325, 2015

be routed to estimate streamflow. The standard version of the JULES model until very recently (February 2015) did not account for a routing mechanism. To overcome this model limitation, we use a conceptual lumped routing approach based on triangular filtering in order to delay runoff response. This is applied after discriminating the gridboxes that contribute to runoff production of a specific basin from the gridded model output. Determination of gridboxes upstream of the gauging station location is implemented using the TRIP river routing scheme (Oki and Sud, 1998).

2.3 Identifying changing climate trends

For the assessment of the impact of the +4 °C warming relative to pre-industrial, the projected time-slices are compared to the baseline period in terms of both absolute and percent change. This is done for each ensemble member individually in order to check the variability of the projected changes and also for the ensemble mean. Two hydrologic indicators are tested, the average and the 10th percentile of runoff production.

Average runoff production is a good and widely used indicator of mean hydrological state of a region. The 10th percentile runoff is considered as a representative indicator of the low flow regime (Prudhomme et al., 2011). Consistent low flows (relative to the mean state) are connected with the formation of hydrological drought conditions. Thus the assessment of the changes in low flows could reveal trends towards more intense or/and often extreme lows in the future hydrological cycle. The impact of high-end climate scenarios on average and 10th percentile runoff is presented both as gridded results at the pan-European scale and aggregated at the basin scale for five major European river basins. The Europe study domain along with information on the catchments tested and their corresponding gauging stations are shown in Fig. 1.

2.4 Examination of drought climatology

Another aspect of our low flow analysis is to assess to changes in drought climatology, i.e. the number of days per year that extreme lows in flow occur. This is here done

HESSD
12, 7267–7325, 2015

at the basin scale, following the threshold level method to identify days of discharge deficiencies. The threshold level method is a widely used tool for drought identification applications (Fleig et al., 2006; Vrochidou et al., 2013). According to this method, drought conditions are characterized as the periods during which discharge falls below a pre-defined threshold level. In our application, the threshold is varying daily and is established as in Prudhomme et al. (2011): for each Julian day k, the 10th percentile of a 31 day window discharge centering at day k is derived, from data of all the years of the baseline period (1976–2005). The daily modelled time-series for the whole period simulated (1971–2100) is compared to the daily varying drought limit, and the number of days that fall below the threshold is summed up on an annual basis. The drought threshold is derived from the flows of the baseline period and is applied to both historical and projected flows, in order to capture the climate change induced changes in drought climatology.

2.5 Bias correction method

In the present study the multi-segment bias correction (MSBC) method is used to correct the precipitation data for its biases. A detailed description of the method can be found in Grillakis et al. (2013). This bias correction methodology has the ability to better transfer the observed precipitation statistics to the raw GCM data. The method utilizes multiple discrete segments on the cumulative density function (CDF) to fit multiple theoretical distributions, as opposed to the commonly used single transfer function at the entire CDF space. Pragmatically, the method eliminates to a large extent the bias in mean precipitation, while significantly reducing the bias of the higher quantile of the precipitation CDF associated with extreme precipitation events.

HESSD
12, 7267–7325, 2015

3 Results

3.1 Hydrological simulation at Pan-European scale with Euro-CORDEX forcing data

Figure 2 shows the average runoff production estimated by JULES forced with the five participating dynamical downscaled GCMs. The change in runoff in the +4 °C projected time-slice with respect to the baseline period is expressed as both absolute and percent relative difference. It is interesting to observe the variations between the models for the historical time-slice, with the low climate sensitivity GFDL and NorESM1 exhibiting generally wetter patterns, especially for northern Europe and Scandinavian Peninsula, and with IPSL describing drier patterns, especially for southern Europe. For the projected time-slice, all models agree in a general pattern of increased runoff production in northern and central Europe and decreased runoff production in the Mediterranean region. Especially for the negative trends shown in southern Europe it is important that though small in absolute terms they increase in magnitude when expressed as a percentage, meaning that small negative changes can pose severe stress in regions where water availability is already an issue. Even more alarming trends are deduced from Fig. 3, which shows the changes in 10th percentile runoff production at +4 °C compared to baseline. The 10th percentile limit is used to describe low flows that are related to the creation of hydrological drought conditions. According to Fig. 3, all models agree in relative decreases in runoff production in western and southern Europe which are specifically pronounced in the western Iberian and Balkan Peninsulas. Another common trend between the models is the significant increase in runoff production in the Scandinavian Peninsula, with MIROC5 being the only ensemble member that expands this wetter climate down to central Europe.

Figures 4 and 5 illustrate the changes in ensemble mean behaviour in the +4 °C time-slice for average and 10th percentile runoff respectively along with the coefficient of variation between the ensemble members, which serves as a measure of model agreement. As can be observed in Fig. 4, less extreme values are encountered in the

HESSD
12, 7267–7325, 2015

ensemble mean of projected changes in runoff, compared to the change projected by each ensemble member individually (Fig. 2). Thus averaging has smoothed out the projected changes, making it easier to identify clear patterns of change. Especially for percent change a clear trend of runoff increase is revealed in northern Europe and decrease in southern Europe, with a mixed pattern for central Europe, all between the range of −50 to 50 %. In contrast, percent change in 10th percentile runoff for the ensemble mean (Fig. 5) shows more significant reductions (up to 100 %), with this trend covering most of the European area. It is thus deduced that the changes in low flows are more pronounced than the changes in the mean, a conclusion that points towards the overall intensification of the water cycle.

Concerning the ensemble members' agreement, for average runoff (Fig. 4) the coefficient of variation is below 0.5 for most of the European region, which indicates a good agreement of the models. The coefficient of variation is lower for the Scandinavian region and is reduced towards the lower latitudes. No significant variations can be observed between the coefficient of variation of the baseline and the projected period. For 10th percentile runoff, model agreement is notably reduced, with the coefficient of variation for most regions exceeding 0.5 while it exceeds the unity for a large part of Europe.

3.2 Hydrological simulation at Pan-European scale with bias adjusted Euro-CORDEX forcing data

The ensemble mean of average runoff derived from the five participating downscaled GCMs, whose temperature and precipitation were bias adjusted according to the WFDEI dataset is presented in Fig. 6. From the ensemble mean runoff for the baseline period it is clear that bias adjustment of the forcing data resulted in a drier hydrological response from the JULES model. The spatial pattern is similar to that of the raw data ensemble but the magnitude is fairly reduced. For the projected change, data bias adjustment has a small but notable effect on the magnitude of the absolute and percent change, with increases in runoff in northern Europe getting more pronounced in the

Discussion Paper | Discussion Paper | Discussion Paper | Discussion Paper |

HESSD

12, 7267–7325, 2015

High-end climate change impact on European water availability and stress

L. V. Papadimitriou et al.

runs after bias correction. For some regions in central Europe, where a small negative change is reported by the raw data run, a sign change of the projected difference is documented after bias correction. Lastly, bias correction has a strong positive effect on model agreement as it can be documented from the low values of the coefficient of determination all over Europe, with the exception of the Scandinavian Peninsula where model disagreement appears increased after bias correction. For the baseline period model agreement is stronger compared to the projected period, especially for southern Europe.

In Fig. 7, the effect of bias correction on the representation of the 10th percentile runoff is shown. As in Fig. 6, a decrease in the historical ensemble mean is observed over the whole European region. Some hotspots of pronounced negative changes in western Europe have been eliminated and replaced with milder projected absolute changes. There are areas where sign change is observed (central and central-west Europe) however it is difficult to interpret this result and correlate it with bias correction as these are also the areas where models show the lowest agreement (coefficient of variation exceeding one). Although the coefficient of variation is considerably reduced compared to the raw data runs, there are still areas of high model uncertainty in the representation of lower flows.

3.3 Basin averaged runoff regime

In Fig. 8, annual time-series of basin averaged runoff production (average and 10th percentile) for five European basins are shown. These cover the whole length of historical and projected years simulated (1971–2100) in an attempt to identify general trends in average and low runoff, calculating 10 year moving averages from the ensemble mean. Results in Fig. 8 include both raw and bias adjusted output, thus an assessment of the effect of the bias correction on the basin scale hydrology can be made. A common observation for all the basins is that runoff decreases considerably for bias adjustment input forcing. For Danube, Rhine and Guadiana, slight negative trends are identified for average runoff, which are more pronounced for the 10th percentile

Discussion Paper | Discussion Paper | Discussion Paper | Discussion Paper |

HESSD

12, 7267–7325, 2015

High-end climate change impact on European water availability and stress

L. V. Papadimitriou et al.

runoff. For Elbe, a clear trend cannot be identified while for Kemijoki average and low flows are both exhibiting increasing trends. Basin scale average annual runoff production for raw and bias adjusted Euro-CORDEX data as well as the +4 °C absolute and percent change for each ensemble member and ensemble mean is included in Table 2. Similar information but for low flows (10th percentile) are presented in the following Table 3.

3.4 Drought climatology at basin scale

Figure 9 shows the results of the drought threshold level method analysis for the five study basins, for raw and bias corrected output. For each year, the number of days under the historical drought threshold has been counted. This allows a comparison of the tendency towards the formation of drought conditions between the historical period and the projected period. As this is a statistically oriented interpretation of our data, we can see that the differences between raw and bias corrected time-series are very small, especially compared to the difference in the magnitude of their absolute values. For Danube, Rhine and Guadiana a clear rising trend can be identified in the 10 year moving average of ensemble mean of days under threshold per year and for Kemijoki a strong decreasing trend is observed. For Elbe a sign in the trend cannot be identified. For Danube, Rhine and Kemijoki the raw and bias corrected moving averages almost completely coincide. For Elbe and Guadiana the moving averages of the raw data exhibit a slightly more intense upward trend. These are the two basins where also the range of the raw and bias corrected data vary the most.

3.5 Impacts of 4 °C warming relative to 2 °C warming

Figure 10 shows the basin average runoff production for raw and bias corrected Euro-CORDEX data with respect to the corresponding SWL in degrees Celsius. This analysis considers the runoff values corresponding to the +2 and +4 °C SWLs, the latter ranging from 3.2 to 4 between the GCMs, and also the SWL achieved by each

HESSD
12, 7267–7325, 2015

participating GCM in the baseline period (0.3–0.5 °C). It is thus allowing us to examine the changes in basin runoff as temperature increases and to compare the effect of different SWLs.

Comparing the annual average runoff production for raw and bias corrected input forcing it is clear that bias corrected output exhibits a considerably reduced range, which translates in increased model agreement for the basins of Danube, Rhine, Elbe and Guadiana. In Kemijoki basin the bias adjusted output has a greater range than the raw output. Concerning the range of the low flows, an increase in model agreement for the bias corrected forcing is observed for all basins.

Examining the changes in annual average runoff, a slight decreasing trend can be identified for Danube and a slight increasing trend for Elbe while for Rhine there is not a clear trend present. In contrast, Guadiana and Kemijoki exhibit strong decreasing and increasing trends respectively. The falling trend in Guadiana is marginally intensified between 2 and 4 SWL compared to 0 to 2 SWL. The rising trend in Kemijoki does not have evident differences between +2 and +4 °C.

The effect of climate warming is far more pronounced for the low flows. According to the results in Fig. 10 the 10th percentile runoff in Danube and Rhine significantly decreases as SWLs increase while the opposite trend is observed for the low flows in Kemijoki. For Elbe, there is not a clear sign in trend for the bias corrected output, in contrast with the raw results that show an intense decreasing trend up to 2 SWL which continues more moderately until 4 SWL. For Guadiana it is difficult to observe a trend in the bias corrected low percentile runoff as the values are already very low. For the raw output however there is a significant decrease from 0 to +2 °C which continues with a milder trend up to +4 °C.

Figure 11 illustrates the correlation between the percent projected change in annual average and 10th percentile runoff production from bias corrected and raw forcing, for the +2 and +4 SWLs.

Concerning the effect of bias adjustment it can be observed that regardless the significant differences in magnitude between runoff from raw and bias corrected data

HESSD
12, 7267–7325, 2015

discussed before, the projected change in average flow by the two forcings almost coincide for the +2 SWL. For the +4 SWL the GCM range has increased for Kemijoki after bias adjustment while for the rest of the basins raw and bias corrected data result in very similar levels of same percent change. For the projected change in 10th percentile runoff, the larger spreading of the values in Fig. 11 (right column) shows that the GCM uncertainty on this field is higher. Guadiana is the only basin where bias corrected data result in an improvement in GCM agreement, probably due to its very low values of 10th percentile runoff. Kemijoki is not included in the 10th percentile scatterplots as its projected increase far exceeds the 100 % limit selected. For the rest of the basins, the effect of the bias correction on the change of the 10th percentile runoff is not constant. For Guadiana and Elbe bias adjustment mostly increases percent change while for Rhine and Danube percent change is in general terms decreased after bias correction.

Comparing the difference on percent projected change in average annual runoff from +2 to +4 SWL it can be observed that temperature increase results in a slight decline in percent change for basins with small absolute values of change, causing sign changes for Danube and Rhine, and it intensifies the negative and positive changes of Guadiana and Kemijoki respectively. For the 10th percentile runoff there is a similar response to temperature increase. For Elbe there is positive percent change at +2 SWL which falls below zero at +4 SWL while for Danube, Rhine and Guadiana the already declining projected changes present are further intensified.

3.6 Effect of observational datasets for bias correction on the output of the hydrological model

The aspect of the impact posed by the observational dataset used for bias correction to the results of the hydrological simulations is introduced in this part of our analysis. Additional model runs performed with bias adjusted Euro-CORDEX precipitation and temperature, corrected against the E-OBS (instead of the WFDEI) dataset participate in a comprehensive comparison between all the outputs used in this study. The results are

HESSD
12, 7267–7325, 2015

illustrated in Fig. 12. Three different sets of outputs are compared: one driven by raw downscaled and two driven by Euro-CORDEX data bias corrected against two different datasets. The comparison considers both the mean and range of the ensembles and results are presented as basin aggregates. The first part of the comparison concerns the long-term annual average for the period 1976–2005 (Fig. 12, top row) and apart from the model results includes values corresponding to observations, derived from GRDC discharge measurements. Observations can serve as a baseline for this comparison, allowing us to evaluate which configuration can better simulate "true" water budget numbers and the effect of bias correction with respect to this baseline.

For all basins the raw data result in overestimates of runoff production which is though significantly reduced after bias correction. E-OBS corrected data however produce values lower than the observations (with the exception of Guadiana) while the WFDEI-corrected data produce the best simulation in terms of approximating the observed values. As already has been revealed in previous stages of this analysis, it is again clear the impact that bias adjustment has on the increase of model agreement. The only exception is Kemijoki basin due to its high latitude position (coefficient of variation was increased after bias correction for the high latitude areas).

Changes in annual average runoff production at the +4 SWL appear to be more intensified compared to the +2 SWL (Fig. 12, middle and bottom). Although for percent change the differences of the distinctive configurations are less pronounced, variations can be observed between the two bias corrected data driven simulations. It is also interesting that the effect of bias correction on reducing the uncertainty is not that strong when looking the results from the more statistical perspective of percent projected change. The improvements in model agreement after bias adjustment however are still significant for all basins except for Rhine.

HESSD
12, 7267–7325, 2015

4 Discussion

4.1 Hydrological response to +4 °C global warming

In our analysis we investigated the effects of climate change on the European hydrological resources, extracting time periods that correspond to an increase of 4 °C of the global temperature, rather than using pre-defined time-slices. The same approach was followed by Vautard et al. (2013), stating that reduced GCM induced uncertainty is achieved with this method and thus the regional patterns of change in the variables of study are strengthened.

The findings of the study regarding the climate changed induced alterations of the mean hydrological state in Europe show decreasing trends for southern Europe, including the Mediterranean region, and strong increasing trends for northern and north-eastern Europe. These follow the same patterns as identified by previous studies. Schneider et al. (2013) found that the most pronounced changes in the magnitude of European river flows are projected for the Mediterranean region and the northern part of the continent. Hagemann et al. (2013) reported positive changes in projected runoff for the high latitudes and negative changes for southern Europe. For central Europe the projected changes are smaller (mostly in the range of −25 to 25 %) and thus more easily obscured by GCM and bias correction uncertainty. Arnell and Lloyd-Hughes (2014) report that the main source of uncertainty in the projected climate impact stems from the GCMs, with a range of uncertainty for the CMIP5 ensemble that is similar to that of older climate model experiments.

The projected relative changes found for 10th percentile runoff are far more pronounced than the changes in average, even for the regions where changes in average-state annual runoff were negligible. This finding implies that seasonality in runoff is likely to intensify under climate change and is in accordance with the results of Fung et al. (2011) and Van Vliet et al. (2013) who also reported pronounced seasonality in their projected simulations. This may translate to increased dry spells and thus elevated drought risks in the future. With the mean-state runoff changing slightly,

HESSD
12, 7267–7325, 2015

and the low-state changing significantly, it is deduced that high-flows are also to be considerably affected by climate change. More extreme hydrological events are hence expected in the future under the light of these findings, concerning both extreme lows (droughts) and highs (floods). It should be noted however that projections of low flow bear higher uncertainty compared to average-state, as indicated by the higher values of the coefficient of variation.

Concerning the effects of a +4 °C temperature increase on the European hydrological regime compared to a +2 °C increase, significant alterations posed by the +2 °C of global warming are identified for south Europe and northern and north-eastern Europe, where the respective decreasing and rising trends are intensified. Fung et al. (2011) also found that changes in mean annual runoff identified at +2 are intensified at +4. More specifically, their study reports that regions where decreasing runoff trends have been found become even drier and, in contrast, areas where runoff is projected to increase are getting wetter. For most of the river basins examined by Fung et al. (2011), water stress is increased at +4 compared to +2, with the exception of a few basins where an increase in rainfall is projected thus decreasing water stress. In our study, the basins located at central Europe (Danube, Rhine and Elbe) do not exhibit significant changes in their annual average runoff values due to temperature increase from +2 to +4. For 10th percentile runoff, however, a temperature increase of +4 °C from the pre-industrial baseline results in an aggravation of the lowering trends that are already significantly affecting the low runoff regime at +2 °C.

From the analysis performed on drought climatology, increased number of days per year under the historically defined drought threshold are found for the basins of Danube, Rhine and Guadiana. Our results correspond with the findings of previous studies about drought regime under climate change. Giuntoli et al. (2015), investigating future high and low flow regimes at the global scale, using multiple impact models and climate scenarios, found increased number of low flow days in Southern Europe. In the study of Wanders and Van Lanen (2015) the impact of climate change on the hydrological drought regime of different climate regions was assessed, using

HESSD
12, 7267–7325, 2015

a conceptual hydrological model forced with 3 GCMs. The study findings describe a decrease in the frequency of drought events in the future, which however does not point towards drought alleviation. In contrast, it relates to increased drought event duration and deficit volume. These effects are more pronounced for the arid climates that already face problems of water availability.

4.2 The effect of bias correction

As proposed by Ehret et al. (2012), both raw and bias corrected data driven simulations are presented in our study, in order to comprehensively assess the effect of bias correction on our results. In four of the five study basins, raw data driven simulated runoff overestimates the corresponding observed values. After bias correction, the modelled results represent more accurately the past hydrological regime. Similar improvements in the bias corrected output have been reported by Hagemann et al. (2011), Muerth et al. (2013) and Harding et al. (2014).

For some regions, the sign of the projected change in runoff shifted after bias correction. This finding was also encountered in the study of Hagemann et al. (2011). Hagemann et al. (2011) underline that these changes in the climate signal reveal another uncertainty aspect of the GCM to GHM modelling procedure, that is inherent to the GCM but becomes apparent after the bias adjustment of the climate model output. Teng et al. (2015) argue that signal changes are produced by bias correction errors in higher percentiles' precipitation, thus adding another factor to the uncertainty of the runoff projections.

Although the absolute values of raw and bias corrected simulations differ significantly, this does not apply to the projected relative changes. Liu et al. (2014) also found that raw and bias corrected data resulted in similar estimations of relative changes for a series a variables, including ET and runoff. The study of Muerth et al. (2013) investigates the effect of bias adjustment on hydrological simulations and their climate change induced alterations. Concerning the relative changes between baseline and

HESSD
12, 7267–7325, 2015

High-end climate change impact on European water availability and stress

L. V. Papadimitriou et al.

future time-slices, it is reported that bias correction does not influence notably the hydrologic indicators, apart from the one describing flow seasonality.

Chen et al. (2011) identify three uncertainty components in bias correction applications: the uncertainty of the different GCM, the variable emission scenarios and that of the decade used for bias adjustment. From a comparison of the latter uncertainty source with the two former, concluded that the choice of correction decade has the smallest contribution to total uncertainty. In this paper we address another uncertainty source; that of the dataset used for correction. It was found that the WFDEI-bias corrected simulation captured better the past hydrological regime compared to the E-OBS-bias corrected configuration. The differences between the two simulations abate when results are expressed as percent change but still their variations are of the same magnitude as that between raw and bias corrected data. This implies that the selection of the observational dataset used for bias correction is not a trivial step of the modelling procedure and it should be treated as an extra factor that causes the uncertainty window of the projected hydrologic conditions to further open.

5 Conclusions

In this paper, the future mean- and low-hydrological states under +4 °C of global warming were assessed for the European region, using the novel dataset of the Euro-CORDEX climate projections. An analysis of the changes in future drought climatology was performed for five major European basins and the impact of +2 vs. +4 °C global warming was estimated. Concurrently, the effect of bias correction of the climate model outputs on the projected climate was also evaluated.

The concluding remarks of this study are summarised below.

Projections show an intensification of the water cycle at +4 SWL, as even for areas where the average state is not considerably affected, there are remarked projected decreases of low flows. With the exception of the Scandinavian Peninsula and some small areas in central Europe, 10th percentile runoff production is projected to reduce

HESSD
12, 7267–7325, 2015

all over Europe. This favours the formation of extreme hydrological events thus more droughts and floods compared to the current state are expected in the future due to the warming climate.

Drought climatology is projected to change to more dry days per year for the Danube, Rhine and Guadiana basins. Thus these areas are projected to experience more usual and more intense drought events in the future.

For the areas where clear decreasing or increasing runoff trends are identified in the projections, these changes are considerably intensified when moving from the +2 to the +4 SWL. Decreasing trends apply to southern Europe, including the Mediterranean region, while strong increasing trends are projected for northern and north-eastern Europe. For the rest of the European region where trends are not clear or ensemble members do not agree towards the change, the effect of the plus two degrees warming does not seem to severely affect the hydrological state, which is however already significantly altered at +2 SWL compared to pre-industrial.

Bias correction results in an improved representation of the historical hydrological conditions. However, raw and bias corrected simulations exhibit minor variations for results of statistical interpretation (in our study: percent change, number of days under drought threshold).

The dataset used for bias correction can affect the quality of the projections in absolute terms to a great extent. The comparison performed here showed that the WFDEI-corrected dataset produces simulations that capture better the past observed hydrologic state compared to the E-OBS-corrected dataset and should thus be preferred for bias correction applications over Europe. The selection of the "correct" dataset is an added uncertainty to the climate impact modelling chain, with magnitude similar to that of the bias correction procedure itself.

Acknowledgements. The research leading to these results has received funding from HELIX project of the European Union's Seventh Framework Programme for research, technological development and demonstration under grant agreement no 603864. We acknowledge the World Climate Research Programme's Working Group on Regional Climate, and the Working

HESSD
12, 7267–7325, 2015
High-end climate change impact on European water availability and stress
L. V. Papadimitriou et al.

Group on Coupled Modelling, former coordinating body of CORDEX and responsible panel for CMIP5. We also thank the climate modelling groups (listed in Table 1 of this paper) for producing and making available their model output. We also acknowledge the Earth System Grid Federation infrastructure an international effort led by the U.S. Department of Energy's Program for Climate Model Diagnosis and Intercomparison, the European Network for Earth System Modelling and other partners in the Global Organisation for Earth System Science Portals (GO-ESSP). Finally, we acknowledge the E-OBS dataset from the EU-FP6 project ENSEMBLES (http://ensembles-eu.metoffice.com) and the data providers in the ECA&D project (http://www.ecad.eu).

References

Alcamo, J., Döll, P., Henrichs, T., Kaspar, F., Lehner, B., Rösch, T., and Siebert, S.: Development and testing of the WaterGAP 2 global model of water use and availability, Hydrolog. Sci. J., 48, 317–337, doi:10.1623/hysj.48.3.317.45290, 2003.

Alfieri, L., Burek, P., Feyen, L., and Forzieri, G.: Global warming increases the frequency of river floods in Europe, Hydrol. Earth Syst. Sci., 19, 2247–2260, doi:10.5194/hess-19-2247-2015, 2015.

Andrews, T., Gregory, J. M., Webb, M. J., and Taylor, K. E.: Forcing, feedbacks and climate sensitivity in CMIP5 coupled atmosphere–ocean climate models, Geophys. Res. Lett., 39, 1–7, doi:10.1029/2012GL051607, 2012.

Arnell, N.: A simple water balance model for the simulation of streamflow over a large geographic domain, J. Hydrol., 217, 314–335, doi:10.1016/S0022-1694(99)00023-2, 1999.

Arnell, N. W. and Gosling, S. N.: The impacts of climate change on river flow regimes at the global scale, J. Hydrol., 486, 351–364, doi:10.1016/j.jhydrol.2013.02.010, 2013.

Arnell, N. W. and Lloyd-Hughes, B.: The global-scale impacts of climate change on water resources and flooding under new climate and socio-economic scenarios, Climatic Change, 122, 127–140, doi:10.1007/s10584-013-0948-4, 2014.

Arnell, N. W., Lowe, J. A., Brown, S., Gosling, S. N., Gottschalk, P., Hinkel, J., Lloyd-Hughes, B., Nicholls, R. J., Osborn, T. J., Osborne, T. M., Rose, G. A., Smith, P., and Warren, R. F.: A global assessment of the effects of climate policy on the impacts of climate change, Nature Climate Change, 3, 512–519, doi:10.1038/nclimate1793, 2013.

HESSD
12, 7267–7325, 2015

Bakopoulou, C., Bulygina, N., Butler, A., and McIntyre, N.: Sensitivity analysis and parameter identifiability of the land surface model JULES at the point scale in permeable catchments, Proc. of British Hydrological Society National Symposium, Dundee, June 2012.

Best, M. J., Pryor, M., Clark, D. B., Rooney, G. G., Essery, R.L. H., Ménard, C. B., Edwards, J. M., Hendry, M. A., Porson, A., Gedney, N., Mercado, L. M., Sitch, S., Blyth, E., Boucher, O., Cox, P. M., Grimmond, C. S. B., and Harding, R. J.: The Joint UK Land Environment Simulator (JULES), model description – Part 1: Energy and water fluxes, Geosci. Model Dev., 4, 677–699, doi:10.5194/gmd-4-677-2011, 2011.

Betts, R. A., Collins, M., Hemming, D. L., Jones, C. D., Lowe, J. A., and Sanderson, M. G.: When could global warming reach 4 °C?, Philos. T. R. Soc. A, 369, 67–84, doi:10.1098/rsta.2010.0292, 2011.

Betts, R. A., Golding, N., Gonzalez, P., Gornall, J., Kahana, R., Kay, G., Mitchell, L., and Wiltshire, A.: Climate and land use change impacts on global terrestrial ecosystems and river flows in the HadGEM2-ES Earth system model using the representative concentration pathways, Biogeosciences, 12, 1317–1338, doi:10.5194/bg-12-1317-2015, 2015.

Beven, K. J. and Kirkby, M. J.: A physically based, variable contributing area model of basin hydrology/Un modèle à base physique de zone d'appel variable de l'hydrologie du bassin Hydrological Sciences Bulletin, 24, 43–69, doi:10.1080/02626667909491834, 1979.

Bonaccorso, B., Peres, D. J., Cancelliere, A., and Rossi, G.: Large scale probabilistic drought characterization over Europe, Water Resour. Manag., 27, 1675–1692, doi:10.1007/s11269-012-0177-z, 2013.

Burke, E. J., Dankers, R., Jones, C. D., and Wiltshire, A. J.: A retrospective analysis of pan Arctic permafrost using the JULES land surface model, Clim. Dynam., 41, 1025–1038, doi:10.1007/s00382-012-1648-x, 2013.

Chen, C., Haerter, J. O., Hagemann, S., and Piani, C.: On the contribution of statistical bias correction to the uncertainty in the projected hydrological cycle, Geophys. Res. Lett., 38, 1–6, doi:10.1029/2011GL049318, 2011.

Ciscar Martinez, J. C., Feyen, L., Soria, A., Lavalle, C., Miles, P., Raes, F., Nemry, F., Demirel, H., Rózsai, M., Dosio, A., Donatelli, M., Srivastava, A. K., Fumagalli, D., Niemeyer, S., Shrestha, S., Ciaian, P., Himics, M., Van Doorslaer, B., Barrios, S., Ibanez Rivas, J. N., Forzieri, G., Rojas Mujica, R. F., Bianchi, A., DOWLING Paul, P., Camia, A., Liberta, G., San-Miguel-Ayanz, J., de Rigo, D., Caudullo, G., Barredo Cano, J. I., Paci, D., Pycroft, J., Saveyn, B., Revesz, T., Baranzelli, C., Vandecasteele, I., Batista E Silva, F., and Ibarreta

HESSD

12, 7267–7325, 2015

High-end climate change impact on European water availability and stress

L. V. Papadimitriou et al.

Ruiz, D.: Climate Impacts in Europe, The JRC PESETA II Project, available from: http://econpapers.repec.org/RePEc:ipt:iptwpa:jrc87011 (last access: 31 July 2015), 2014.
Clark, D. B., Mercado, L. M., Sitch, S., Jones, C. D., Gedney, N., Best, M. J., Pryor, M., Rooney, G. G., Essery, R. L. H., Blyth, E., Boucher, O., Harding, R. J., Huntingford, C., and Cox, P. M.: The Joint UK Land Environment Simulator (JULES), model description – Part 2: Carbon fluxes and vegetation dynamics, Geosci. Model Dev., 4, 701–722, doi:10.5194/gmd-4-701-2011, 2011.
Cox, P. M., Huntingford, C., and Harding, R. J.: A canopy conductance and photosynthesis model for use in a GCM land surface scheme, J. Hydrol., 212–213, 79–94, doi:10.1016/S0022-1694(98)00203-0, 1998.
Cox, P. M.: Description of the TRIFFID dynamic global vegetation model, Hadley Centre, United Kingdom Meteorological Office, Bracknell, UK, Technical Note 24, 2001.
Dadson, S. J., Ashpole, I., Harris, P., Davies, H. N., Clark, D. B., Blyth, E., and Taylor, C. M.: Wetland inundation dynamics in a model of land surface climate: evaluation in the Niger inland delta region, J. Geophys. Res., 115, D23114, doi:10.1029/2010JD014474, 2010.
Dankers, R., Burke, E. J., and Price, J.: Simulation of permafrost and seasonal thaw depth in the JULES land surface scheme, The Cryosphere, 5, 773–790, doi:10.5194/tc-5-773-2011, 2011.
Dankers, R., Arnell, N. W., Clark, D. B., Falloon, P. D., Fekete, B. M., Gosling, S. N., Heinke, J., Kim, H., Masaki, Y., Satoh, Y., Stacke, T., Wada, Y., and Wisser, D.: First look at changes in flood hazard in the Inter-Sectoral Impact Model Intercomparison Project ensemble, P. Natl. Acad. Sci. USA, 111, 3257–3261, doi:10.1073/pnas.1302078110, 2014.
Döll, P. and Schmied, H. M.: How is the impact of climate change on river flow regimes related to the impact on mean annual runoff? A global-scale analysis, Environ. Res. Lett., 7, 014037, doi:10.1088/1748-9326/7/1/014037, 2012.
Döll, P., Kaspar, F., and Lehner, B.: A global hydrological model for deriving water availability indicators: model tuning and validation, J. Hydrol., 270, 105–134, doi:10.1016/S0022-1694(02)00283-4, 2003.
Ehret, U., Zehe, E., Wulfmeyer, V., Warrach-Sagi, K., and Liebert, J.: HESS Opinions "Should we apply bias correction to global and regional climate model data?", Hydrol. Earth Syst. Sci., 16, 3391–3404, doi:10.5194/hess-16-3391-2012, 2012.
England, M. H., Kajtar, J. B., and Maher, N.: Robust warming projections despite the recent hiatus, Nature Climate Change, 5, 394–396, doi:10.1038/nclimate2575, 2015.

HESSD
12, 7267–7325, 2015

High-end climate change impact on European water availability and stress

L. V. Papadimitriou et al.

Fischer, E. M. and Knutti, R.: Anthropogenic contribution to global occurrence of heavy-precipitation and high-temperature extremes, Nature Climate Change, 5, 1–6, doi:10.1038/nclimate2617, 2015.
Fleig, A. K., Tallaksen, L. M., Hisdal, H., and Demuth, S.: A global evaluation of streamflow drought characteristics, Hydrol. Earth Syst. Sci., 10, 535–552, doi:10.5194/hess-10-535-2006, 2006.
Flörke, M., Kynast, E., Bärlund, I., Eisner, S., Wimmer, F., and Alcamo, J.: Domestic and industrial water uses of the past 60 years as a mirror of socio-economic development: a global simulation study, Global Environ. Chang., 23, 144–156, doi:10.1016/j.gloenvcha.2012.10.018, 2013.
Forzieri, G., Feyen, L., Rojas, R., Flörke, M., Wimmer, F., and Bianchi, A.: Ensemble projections of future streamflow droughts in Europe, Hydrol. Earth Syst. Sci., 18, 85–108, doi:10.5194/hess-18-85-2014, 2014.
Fung, F., Lopez, A., and New, M.: Water availability in +2 °C and +4 °C worlds, Philos. T. R. Soc. A, 369, 99–116, doi:10.1098/rsta.2010.0293, 2011.
Giuntoli, I., Vidal, J.-P., Prudhomme, C., and Hannah, D. M.: Future hydrological extremes: the uncertainty from multiple global climate and global hydrological models, Earth Syst. Dynam., 6, 267–285, doi:10.5194/esd-6-267-2015, 2015.
Gosling, S. N. and Arnell, N. .: A global assessment of the impact of climate change on water scarcity, Climatic Change, 1–15, doi:10.1007/s10584-013-0853-x, 2013
Grillakis, M. G., Koutroulis, A. G., and Tsanis, I. K.: Multisegment statistical bias correction of daily GCM precipitation output, J. Geophys. Res.-Atmos., 118, 3150–3162, doi:10.1002/jgrd.50323, 2013.
Haddeland, I., Clark, D. B., Franssen, W., Ludwig, F., Voß, F., Arnell, N. W., Bertrand, N., Best, M., Folwell, S., Gerten, D., Gomes, S., Gosling, S. N., Hagemann, S., Hanasaki, N., Harding, R., Heinke, J., Kabat, P., Koirala, S., Oki, T., Polcher, J., Stacke, T., Viterbo, P., Weedon, G. P., and Yeh, P.: Multimodel estimate of the global terrestrial water balance: setup and first results, J. Hydrometeorol., 12, 869–884, doi:10.1175/2011JHM1324.1, 2011.
Haddeland, I., Heinke, J., Biemans, H., Eisner, S., Flörke, M., Hanasaki, N., Konzmann, M., Ludwig, F., Masaki, Y., Schewe, J., Stacke, T., Tessler, Z. D., Wada, Y., and Wisser, D.: Global water resources affected by human interventions and climate change, P. Natl. Acad. Sci. USA, 111, 3251–3256, doi:10.1073/pnas.1222475110, 2014.

Haerter, J. O., Hagemann, S., Moseley, C., and Piani, C.: Climate model bias correction and the role of timescales, Hydrol. Earth Syst. Sci., 15, 1065–1079, doi:10.5194/hess-15-1065-2011, 2011.
Hagemann, S., Chen, C., Haerter, J. O., Heinke, J., Gerten, D., and Piani, C.: Impact of a statistical bias correction on the projected hydrological changes obtained from three GCMs and two hydrology models, J. Hydrometeorol., 12, 556–578, doi:10.1175/2011JHM1336.1, 2011.
Hagemann, S., Chen, C., Clark, D. B., Folwell, S., Gosling, S. N., Haddeland, I., Hanasaki, N., Heinke, J., Ludwig, F., Voss, F., and Wiltshire, A. J.: Climate change impact on available water resources obtained using multiple global climate and hydrology models, Earth Syst. Dynam., 4, 129–144, doi:10.5194/esd-4-129-2013, 2013.
Hanasaki, N., Kanae, S., Oki, T., Masuda, K., Motoya, K., Shirakawa, N., Shen, Y., and Tanaka, K.: An integrated model for the assessment of global water resources – Part 1: Model description and input meteorological forcing, Hydrol. Earth Syst. Sci., 12, 1007–1025, doi:10.5194/hess-12-1007-2008, 2008.
Hanasaki, N., Inuzuka, T., Kanae, S., and Oki, T.: An estimation of global virtual water flow and sources of water withdrawal for major crops and livestock products using a global hydrological model, J. Hydrol., 384, 232–244, doi:10.1016/j.jhydrol.2009.09.028, 2010.
Hanasaki, N., Fujimori, S., Yamamoto, T., Yoshikawa, S., Masaki, Y., Hijioka, Y., Kainuma, M., Kanamori, Y., Masui, T., Takahashi, K., and Kanae, S.: A global water scarcity assessment under Shared Socio-economic Pathways – Part 2: Water availability and scarcity, Hydrol. Earth Syst. Sci., 17, 2393–2413, doi:10.5194/hess-17-2393-2013, 2013.
Harding, R. J., Weedon, G. P., van Lanen, H. A. J., and Clark, D. B.: The future for global water assessment, J. Hydrol., 518, 186–193, doi:10.1016/j.jhydrol.2014.05.014, 2014.
Haylock, M. R., Hofstra, N., Klein Tank, A. M. G., Klok, E. J., Jones, P. D., and New, M.: A European daily high-resolution gridded dataset of surface temperature and precipitation, J. Geophys. Res., 113, D20119, doi:10.1029/2008JD010201, 2008.
Hejazi, M., Edmonds, J., Clarke, L., Kyle, P., Davies, E., Chaturvedi, V., Wise, M., Patel, P., Eom, J., Calvin, K., Moss, R., and Kim, S.: Long-term global water projections using six socioeconomic scenarios in an integrated assessment modeling framework, Technol. Forecast. Soc., 81, 205–226, doi:10.1016/j.techfore.2013.05.006, 2014.

HESSD
12, 7267–7325, 2015

High-end climate change impact on European water availability and stress

L. V. Papadimitriou et al.

Jiménez, C., Clark, D. B., Kolassa, J., Aires, F., and Prigent, C.: A joint analysis of modeled soil moisture fields and satellite observations, J. Geophys. Res.-Atmos., 118, 6771–6782, doi:10.1002/jgrd.50430, 2013.

Laizé, C. L. R., Acreman, M. C., Schneider, C., Dunbar, M. J., Houghton-Carr, H. A., Florke, M., and Hannah, D. M.: Projected flow alteration and ecological risk for pan-european rivers, River Res. Appl., 30, 299–314, doi:10.1002/rra.2645, 2013.

Liu, M., Rajagopalan, K., Chung, S. H., Jiang, X., Harrison, J., Nergui, T., Guenther, A., Miller, C., Reyes, J., Tague, C., Choate, J., Salathé, E. P., Stöckle, C. O., and Adam, J. C.: What is the importance of climate model bias when projecting the impacts of climate change on land surface processes?, Biogeosciences, 11, 2601–2622, doi:10.5194/bg-11-2601-2014, 2014.

MacKellar, N. C., Dadson, S. J., New, M., and Wolski, P.: Evaluation of the JULES land surface model in simulating catchment hydrology in Southern Africa, Hydrol. Earth Syst. Sci. Discuss., 10, 11093–11128, doi:10.5194/hessd-10-11093-2013, 2013.

Marthews, T. R., Malhi, Y., Girardin, C. A. J., Silva Espejo, J. E., Aragão, L. E. O. C., Metcalfe, D. B., Rapp, J. M., Mercado, L. M., Fisher, R. A., Galbraith, D. R., Fisher, J. B., Salinas-Revilla, N., Friend, A. D., Restrepo-Coupe, N., and Williams, R. J.: Simulating forest productivity along a neotropical elevational transect: temperature variation and carbon use efficiency, Glob. Change Biol., 18, 2882–2898, doi:10.1111/j.1365-2486.2012.02728.x, 2012.

Moore, R. J.: The probability-distributed principle and runoff production at point and basin scales, Hydrolog. Sci. J., 30, 273–297, doi:10.1080/02626668509490989, 1985.

Muerth, M. J., Gauvin St-Denis, B., Ricard, S., Velázquez, J. A., Schmid, J., Minville, M., Caya, D., Chaumont, D., Ludwig, R., and Turcotte, R.: On the need for bias correction in regional climate scenarios to assess climate change impacts on river runoff, Hydrol. Earth Syst. Sci., 17, 1189–1204, doi:10.5194/hess-17-1189-2013, 2013.

Oki, T. and Sud, Y. C.: Design of Total Runoff Integrating Pathways (TRIP) – a global river channel network, Earth Interact., 2, 1–37, 1998.

Parry, S., Hannaford, J., Lloyd-Hughes, B., and Prudhomme, C.: Multi-year droughts in Europe: analysis of development and causes, Hydrol. Res., 43, 689–706, 2012.

Penman, H. L.: Natural evaporation from open water, bare soil and grass, P. Roy. Soc. Lond. A Mat., 193, 120–145, 1948.

HESSD

12, 7267–7325, 2015

High-end climate change impact on European water availability and stress

L. V. Papadimitriou et al.

Prudhomme, C., Parry, S., Hannaford, J., Clark, D. B., Hagemann, S., and Voss, F.: How well do large-scale models reproduce regional hydrological extremes in Europe?, J. Hydrometeorol., 12, 1181–1204, doi:10.1175/2011JHM1387.1, 2011.
Prudhomme, C., Giuntoli, I., Robinson, E. L., Clark, D. B., Arnell, N. W., Dankers, R., Fekete, B. M., Franssen, W., Gerten, D., Gosling, S. N., Hagemann, S., Hannah, D. M., Kim, H., Masaki, Y., Satoh, Y., Stacke, T., Wada, Y., and Wisser, D.: Hydrological droughts in the 21st century, hotspots and uncertainties from a global multimodel ensemble experiment, P. Natl. Acad. Sci. USA, 111, 3262–3267, doi:10.1073/pnas.1222473110, 2014.
Pryor, M., Clark, D., Harris, P., and Hendry, M.: Joint UK Land Environment Simulator (JULES) Version 3.2 User Manual, NERC/Centre for Ecology and Hydrology, available at: https://jules.jchmr.org/software-and-documentation/previous-releases/jules-v3.2/downloads/jules_v3.2_users_guide.pdf (last access: 31 July 2015), 2012.
Richards, L. A.: Capillary conduction of liquids through porous mediums, J. Appl. Phys., 1, 318–333, 1931.
Sanford, T., Frumhoff, P. C., Luers, A., and Gulledge, J.: The climate policy narrative for a dangerously warming world, Nature Climate Change, 4, 164–166, 2014.
Schewe, J., Heinke, J., Gerten, D., Haddeland, I., Arnell, N. W., Clark, D. B., Dankers, R., Eisner, S., Fekete, B. M., Colón-González, F. J., Gosling, S. N., Kim, H., Liu, X., Masaki, Y., Portmann, F. T., Satoh, Y., Stacke, T., Tang, Q., Wada, Y., Wisser, D., Albrecht, T., Frieler, K., Piontek, F., Warszawski, L., and Kabat, P.: Multimodel assessment of water scarcity under climate change, P. Natl. Acad. Sci. USA, 111, 3245–3250, doi:10.1073/pnas.1222460110, 2014.
Schneider, C., Laizé, C. L. R., Acreman, M. C., and Flörke, M.: How will climate change modify river flow regimes in Europe?, Hydrol. Earth Syst. Sci., 17, 325–339, doi:10.5194/hess-17-325-2013, 2013.
Teng, J., Potter, N. J., Chiew, F. H. S., Zhang, L., Wang, B., Vaze, J., and Evans, J. P.: How does bias correction of regional climate model precipitation affect modelled runoff?, Hydrol. Earth Syst. Sci., 19, 711–728, doi:10.5194/hess-19-711-2015, 2015.
Teutschbein, C. and Seibert, J.: Bias correction of regional climate model simulations for hydrological climate-change impact studies: review and evaluation of different methods, J. Hydrol., 456–457, 12–29, doi:10.1016/j.jhydrol.2012.05.052, 2012.
Van den Hoof, C., Vidale, P. L., Verhoef, A., and Vincke, C.: Improved evaporative flux partitioning and carbon flux in the land surface model JULES: impact on the simulation

HESSD
12, 7267–7325, 2015

of land surface processes in temperate Europe, Agr. Forest Meteorol., 181, 108–124, doi:10.1016/j.agrformet.2013.07.011, 2013.
Van Huijgevoort, M. H. J., Hazenberg, P., van Lanen, H. A. J., Teuling, A. J., Clark, D. B., Folwell, S., Gosling, S. N., Hanasaki, N., Heinke, J., Koirala, S., Stacke, T., Voss, F., Sheffield, J., and Uijlenhoet, R.: Global multimodel analysis of drought in runoff for the second half of the Twentieth Century, J. Hydrometeorol., 14, 1535–1552, doi:10.1175/JHM-D-12-0186.1, 2013.
Van Vliet, M. T. H., Franssen, W. H. P., Yearsley, J. R., Ludwig, F., Haddeland, I., Lettenmaier, D. P., and Kabat, P.: Global river discharge and water temperature under climate change, Global Environ. Chang., 23, 450–464, doi:10.1016/j.gloenvcha.2012.11.002, 2013.
Vautard, R., Gobiet, A., Jacob, D., Belda, M., Colette, A., Déqué, M., Fernández, J., García-Díez, M., Goergen, K., Güttler, I., Halenka, T., Karacostas, T., Katragkou, E., Keuler, K., Kotlarski, S., Mayer, S., van Meijgaard, E., Nikulin, G., Patarčić, M., Scinocca, J., Sobolowski, S., Suklitsch, M., Teichmann, C., Warrach-Sagi, K., Wulfmeyer, V., and Yiou, P.: The simulation of European heat waves from an ensemble of regional climate models within the EURO-CORDEX project, Clim. Dynam., 41, 2555–2575, doi:10.1007/s00382-013-1714-z, 2013.
Vautard, R., Gobiet, A., Sobolowski, S., Kjellström, E., Stegehuis, A., Watkiss, P., Mendlik, T., Landgren, O., Nikulin, G., Teichmann, C., and Jacob, D.: The European climate under a 2 °C global warming, Environ. Res. Lett., 9, 034006, doi:10.1088/1748-9326/9/3/034006, 2014.
Verzano, K.: Climate change impacts on flood related hydrological processes: further development and application of a global scale hydrological model, University of Kassel, Kassel, 2009.
Vicente-Serrano, S. M., Lopez-Moreno, J.-I., Beguería, S., Lorenzo-Lacruz, J., Sanchez-Lorenzo, A., García-Ruiz, J. M., Azorin-Molina, C., Morán-Tejeda, E., Revuelto, J., Trigo, R., Coelho, F., and Espejo, F.: Evidence of increasing drought severity caused by temperature rise in southern Europe, Environ. Res. Lett., 9, 044001, doi:10.1088/1748-9326/9/4/044001, 2014.
Vrochidou, A. E. K., Tsanis, I. K., Grillakis, M. G., and Koutroulis, A. G.: The impact of climate change on hydrometeorological droughts at a basin scale, J. Hydrol., 476, 290–301, doi:10.1016/j.jhydrol.2012.10.046, 2013.
Wanders, N. and Van Lanen, H. A. J.: Future discharge drought across climate regions around the world modelled with a synthetic hydrological modelling approach forced by three general

circulation models, Nat. Hazards Earth Syst. Sci., 15, 487–504, doi:10.5194/nhess-15-487-2015, 2015.

Warszawski, L., Frieler, K., Huber, V., Piontek, F., Serdeczny, O., and Schewe, J.: The Inter-Sectoral Impact Model Intercomparison Project (ISI–MIP): project framework, P. Natl. Acad. Sci. USA, 111, 3228–3232, 2014.

Weedon, G. P., Gomes, S., Viterbo, P., Österle, H., Adam, J. C., Bellouin, N., Boucher, O., and Best, M.: The WATCH forcing data 1958–2001: a meteorological forcing dataset for land surface and hydrological models, WATCH Technical Report, 22, 41 pp., 2010.

Weedon, G. P., Balsamo, G., Bellouin, N., Gomes, S., Best, M. J., and Viterbo, P.: The WFDEI meteorological forcing data set: WATCH Forcing Data methodology applied to ERA-Interim reanalysis data, Water Resour. Res., 50, 7505–7514, doi:10.1002/2014WR015638, 2014.

Zulkafli, Z., Buytaert, W., Onof, C., Lavado, W., and Guyot, J. L.: A critical assessment of the JULES land surface model hydrology for humid tropical environments, Hydrol. Earth Syst. Sci., 17, 1113–1132, doi:10.5194/hess-17-1113-2013, 2013.

HESSD

12, 7267–7325, 2015

High-end climate change impact on European water availability and stress

L. V. Papadimitriou et al.

Table 1. Euro-CORDEX climate scenarios used to force JULES.

	RCM	GCM	Time-slice closer to +4 °C	Exceeded warming level (°C) in the time-slice	Equilibrium climate sensitivity (K)
1	RCA4	GFDL-ESM2M	2071–2100	3.2	2.44
2	RCA4	NorESM1	2071–2100	3.75	2.80
3	RCA4	MIROC5	2071–2100	3.76	2.72
4	RCA4	IPSL-CM5A	2055–2084	4	4.13
5	RCA4	HadGEM2-ES	2060–2089	4	4.59

HESSD
12, 7267–7325, 2015

HESSD
12, 7267–7325, 2015

Table 2. Basin's annual average runoff production for raw and bias adjusted Euro-CORDEX data.

	Basin's Annual Average Runoff Production [mm year^{-1}]											
	Raw						Bias Corrected					
	Historical average 1976–2005						Historical average 1976–2005					
Danube	462.05	362.35	383.78	304.02	266.21	355.68	219.37	249.80	201.95	226.70	229.00	225.36
Rhine	794.21	845.83	616.94	710.16	495.99	692.63	426.67	503.68	415.00	439.11	470.29	450.95
Elbe	371.88	356.72	219.68	337.42	174.41	292.02	148.70	203.39	135.98	174.79	202.12	173.00
Guadiana	166.13	71.44	116.14	46.60	81.51	96.36	93.14	96.42	90.06	79.22	89.82	89.73
Kemijoki	428.17	482.28	427.95	418.03	507.48	452.78	174.68	327.78	197.30	238.28	450.70	277.75
RCM-GCM	RCA4-GFDL-ESM2M +3.2 (2071–2100)	RCA4-NorESM1 +3.75 (2071–2100)	RCA4-MIROC5 +3.76 (2071–2100)	RCA4-IPSL-CM5A +4 (2055–2084)	RCA4-HadGEM2-ES +4 (2060–2089)	MEAN	RCA4-GFDL-ESM2M +3.2 (2071–2100)	RCA4-NorESM1 +3.75 (2071–2100)	RCA4-MIROC5 +3.76 (2071–2100)	RCA4-IPSL-CM5A +4 (2055–2084)	RCA4-HadGEM2-ES +4 (2060–2089)	MEAN
	Absolute change						Absolute change					
Danube	−54.57	3.36	−13.20	−42.04	−14.96	−24.28	−11.83	−1.38	3.61	−30.04	−11.48	−10.22
Rhine	59.95	−19.81	−13.23	−39.31	−20.14	−6.51	53.83	−5.91	6.09	−44.17	−21.73	−2.37
Elbe	2.05	33.91	30.00	−28.39	19.05	11.32	22.81	33.28	31.55	−5.57	25.71	21.55
Guadiana	−55.70	−37.02	−17.16	−14.09	−46.16	−34.03	−26.23	−48.81	−10.37	−28.52	−45.23	−31.83
Kemijoki	146.86	67.46	67.48	174.94	108.26	113.00	149.69	97.38	89.71	179.15	119.97	127.18
	Percent change						Percent change					
Danube	−11.81	0.93	−3.44	−13.83	−5.62	−6.83	−5.39	−0.55	1.79	−13.25	−5.01	−4.54
Rhine	7.55	−2.34	−2.14	−5.54	−4.06	−0.94	12.62	−1.17	1.47	−10.06	−4.62	−0.53
Elbe	0.55	9.51	13.66	−8.42	10.92	3.88	15.34	16.36	23.20	−3.19	12.72	12.46
Guadiana	−33.53	−51.82	−14.78	−30.24	−56.63	−35.31	−28.16	−50.63	−11.51	−36.00	−50.35	−35.47
Kemijoki	34.30	13.99	15.77	41.85	21.33	24.96	85.69	29.71	45.47	75.19	26.62	45.79

Table 3. Basin's 10th percentile of runoff production, derived on an annual basis, for raw and bias adjusted Euro-CORDEX data.

	Basin's 10th percentile on annual basis [mm year^{-1}]											
	Raw						Bias Corrected					
	Historical average 1976–2005						Historical average 1976–2005					
Danube	146.63	96.81	80.55	79.71	58.69	92.48	31.49	41.73	28.54	30.32	37.94	34.00
Rhine	250.22	258.37	162.58	200.59	109.23	196.20	98.23	120.41	93.24	101.58	107.68	104.23
Elbe	118.79	99.15	29.98	98.30	28.95	75.04	10.22	20.08	11.23	16.75	22.14	16.08
Guadiana	0.74	0.00	0.12	0.00	0.00	0.17	0.00	0.00	0.00	0.00	0.00	0.00
Kemijoki	0.80	4.50	1.10	1.47	10.79	3.73	0.25	5.91	0.53	1.00	11.60	3.86
RCM-GCM	RCA4-GFDL-ESM2M +3.2 (2071–2100)	RCA4-NorESM1 +3.75 (2071–2100)	RCA4-MIROC5 +3.76 (2071–2100)	RCA4-IPSL-CM5A +4 (2055–2084)	RCA4-HadGEM2-ES +4 (2060–2089)	MEAN	RCA4-GFDL-ESM2M +3.2 (2071–2100)	RCA4-NorESM1 +3.75 (2071–2100)	RCA4-MIROC5 +3.76 (2071–2100)	RCA4-IPSL-CM5A +4 (2055–2084)	RCA4-HadGEM2-ES +4 (2060–2089)	MEAN
	Absolute change						Absolute change					
Danube	−53.89	−23.89	−18.83	−38.22	−27.41	−32.45	−18.03	−15.89	−9.68	−22.28	−24.37	−18.05
Rhine	−89.38	−87.03	−20.39	−103.94	−43.25	−68.80	−31.43	−49.93	−19.49	−69.92	−52.57	−44.67
Elbe	−29.14	−21.01	1.21	−44.80	−9.96	−20.74	−2.03	−2.73	−0.91	−8.90	−8.52	−4.62
Guadiana	−0.73	0.00	−0.11	0.00	0.00	−0.17	0.00	0.00	0.00	0.00	0.00	0.00
Kemijoki	16.77	53.16	36.71	56.80	72.44	47.18	3.24	3.12	5.05	22.55	16.79	10.15
	Percent change						Percent change					
Danube	−36.75	−24.68	−23.38	−47.95	−46.71	−35.09	−57.26	−38.07	−33.90	−73.50	−64.22	−53.08
Rhine	−35.72	−33.68	−12.54	−51.82	−39.59	−35.07	−32.00	−41.46	−20.91	−68.83	−48.82	−42.86
Elbe	−24.53	−21.19	4.04	−45.57	−34.41	−27.64	−19.86	−13.58	−8.11	−53.15	−38.47	−28.71
Guadiana	−98.67	−73.37	−96.24	−26.22	−76.38	−98.01	−48.53	−50.67	−65.42	−32.31	−56.63	−53.36
Kemijoki	2088.40	1181.25	3328.72	3877.01	671.51	1264.16	1283.66	52.88	946.08	2265.11	144.71	263.09

HESSD
12, 7267–7325, 2015

High-end climate change impact on European water availability and stress

L. V. Papadimitriou et al.

Title Page
Abstract | Introduction
Conclusions | References
Tables | Figures
◂◂ | ▸▸
◂ | ▸
Back | Close
Full Screen / Esc
Printer-friendly Version
Interactive Discussion

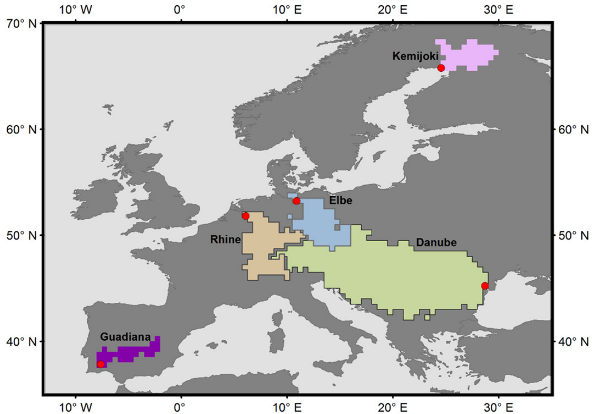

Station Info							
River	**Station**	**GRDC Station No**	**Latitude (dec. degrees)**	**Longitude (dec. degrees)**	**Observed cathment area [km^2]**	**Modelled cathment area [km^2]**
Danube	Ceatal Izmail	6742900	45.22	28.72	807000	815063
Rhine	Rees	6335020	51.75	6.40	159300	177339
Elbe	Neu-Darchau	6340110	53.23	10.89	131950	133886
Guadiana	Pulo do Lovo	6116200	37.82	-7.63	60883	72215
Kemijoki	Isohaara	6854700	65.78	24.55	50686	55628

Figure 1. European study domain, tested basins as defined by the model's 0.5° resolution, gauging stations and general information on the stations.

HESSD
12, 7267–7325, 2015
High-end climate change impact on European water availability and stress
L. V. Papadimitriou et al.

Title Page
Abstract Introduction
Conclusions References
Tables Figures
◀ ▶
◀ ▶
Back Close
Full Screen / Esc
Printer-friendly Version
Interactive Discussion

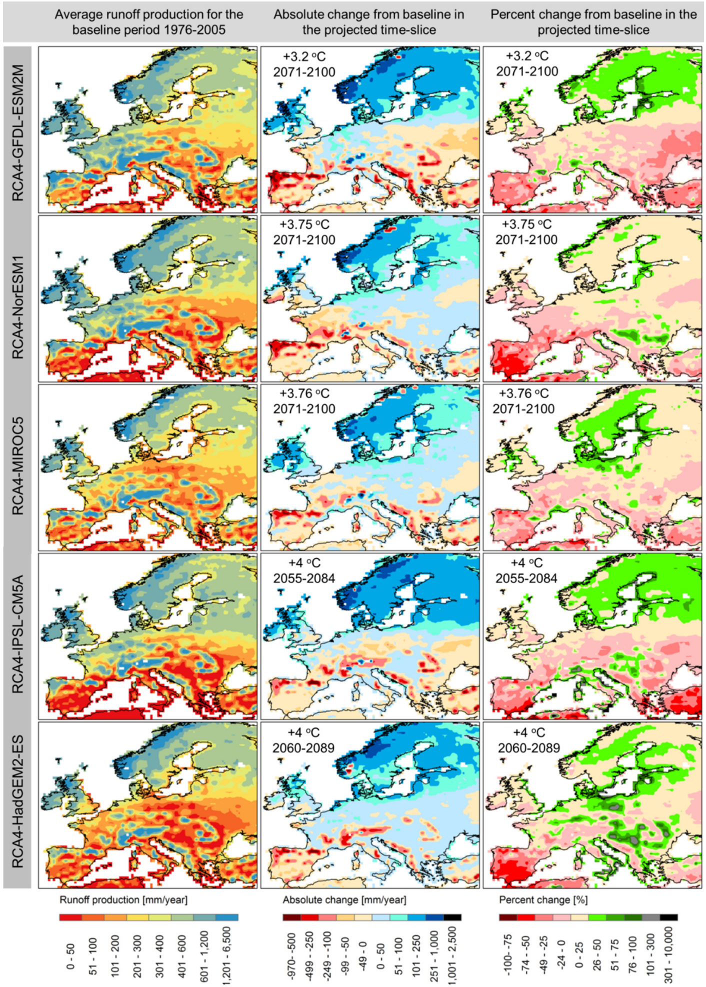

HESSD
12, 7267–7325, 2015

High-end climate change impact on European water availability and stress

L. V. Papadimitriou et al.

Title Page
Abstract | Introduction
Conclusions | References
Tables | Figures
◀ | ▶
◀ | ▶
Back | Close
Full Screen / Esc
Printer-friendly Version
Interactive Discussion

Figure 2. Average runoff production from Euro-CORDEX data for all dynamical downscaled GCMs. Runoff production averaged over the baseline period (1976–2005) (left column), absolute change in runoff in the projected time-slice (middle column) and percent change in the projected time-slice (right column).

HESSD
12, 7267–7325, 2015

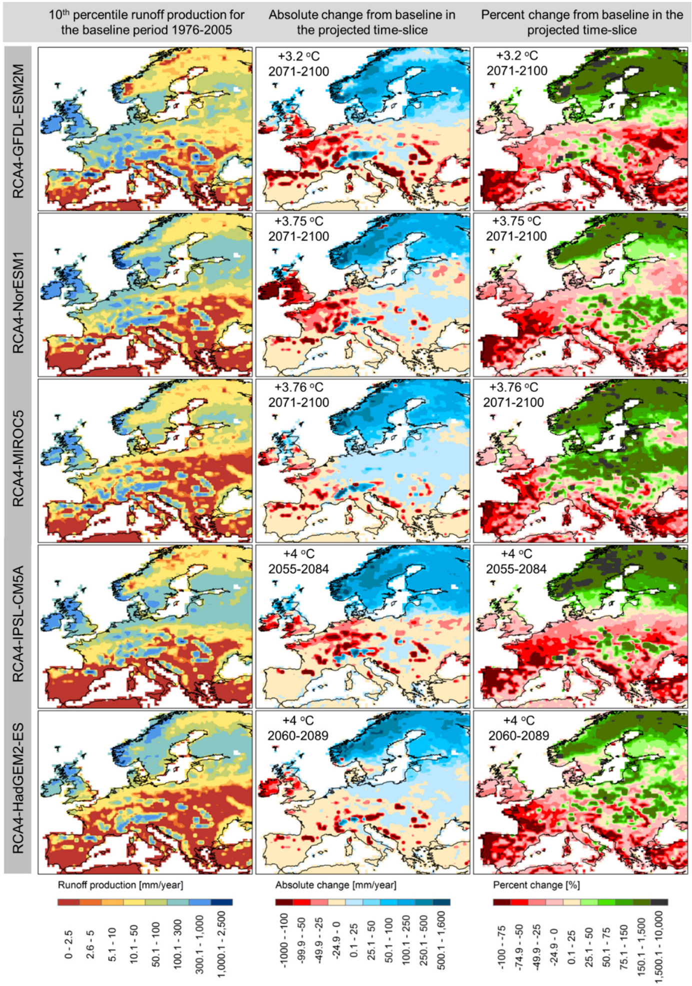

HESSD
12, 7267–7325, 2015

High-end climate change impact on European water availability and stress

L. V. Papadimitriou et al.

Figure 3. 10th percentile of runoff production from Euro-CORDEX data for all dynamical downscaled GCMs. 10th percentile runoff production derived on an annual basis and averaged over the baseline period (1976–2005) (left column), absolute change in 10th percentile runoff in the projected time-slice (middle column) and percent change in the projected time-slice (right column).

HESSD
12, 7267–7325, 2015

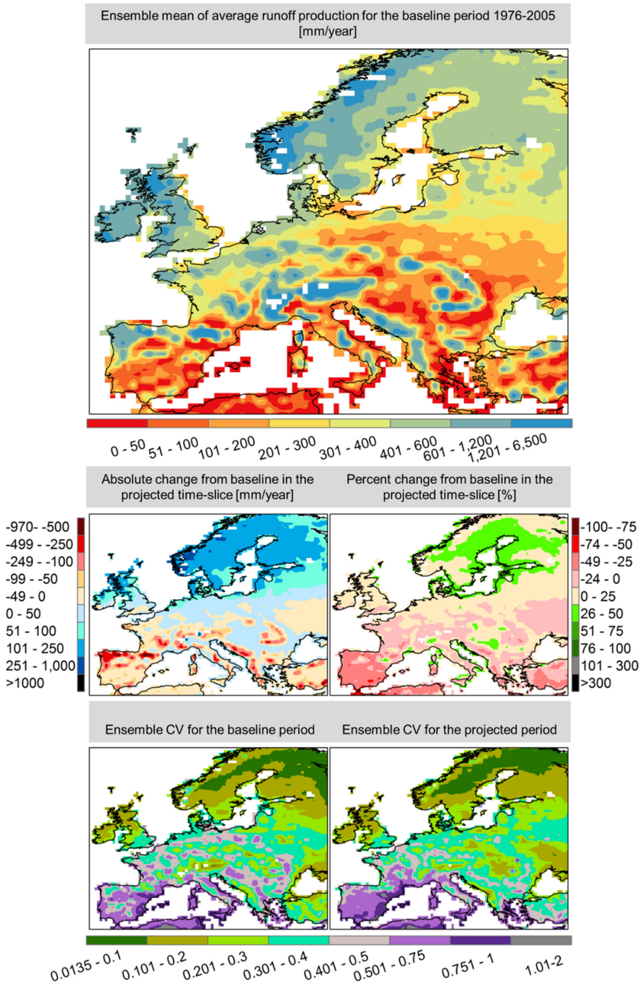

HESSD
12, 7267–7325, 2015

Figure 4. Ensemble mean of average runoff production based on Euro-CORDEX datasets. Runoff production averaged over the baseline period (1976–2005) (top row), absolute and percent change in ensemble mean runoff in the projected time-slice (middle row), coefficient of variation of the ensemble members for the baseline and projected period (bottom row).

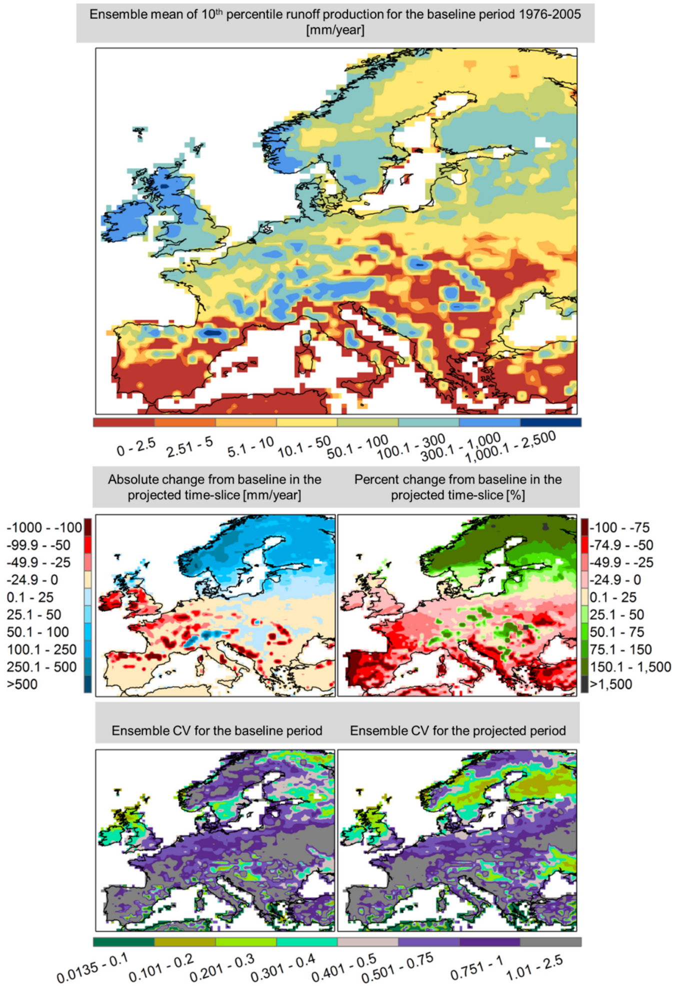

HESSD
12, 7267–7325, 2015

Figure 5. Ensemble mean of 10th percentile runoff production based on Euro-CORDEX datasets. 10th percentile runoff production derived on an annual basis averaged over the baseline period (1976–2005) (top row), absolute and percent change in ensemble mean of 10th percentile runoff in the projected time-slice (middle row), coefficient of variation of the ensemble members for the baseline and projected period (bottom row).

HESSD
12, 7267–7325, 2015

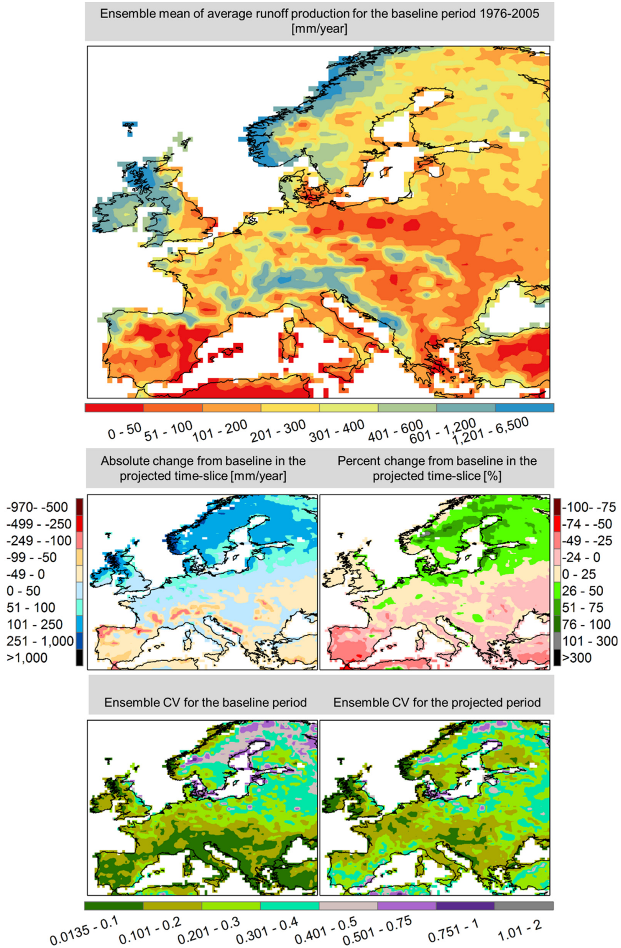

Figure 6. As in Fig. 3, but for bias adjusted Euro-CORDEX data (precipitation and temperature) against WFDEI data.

HESSD
12, 7267–7325, 2015

Title Page
Abstract | Introduction
Conclusions | References
Tables | Figures
◀| |▶
◀ ▶
Back | Close
Full Screen / Esc
Printer-friendly Version
Interactive Discussion

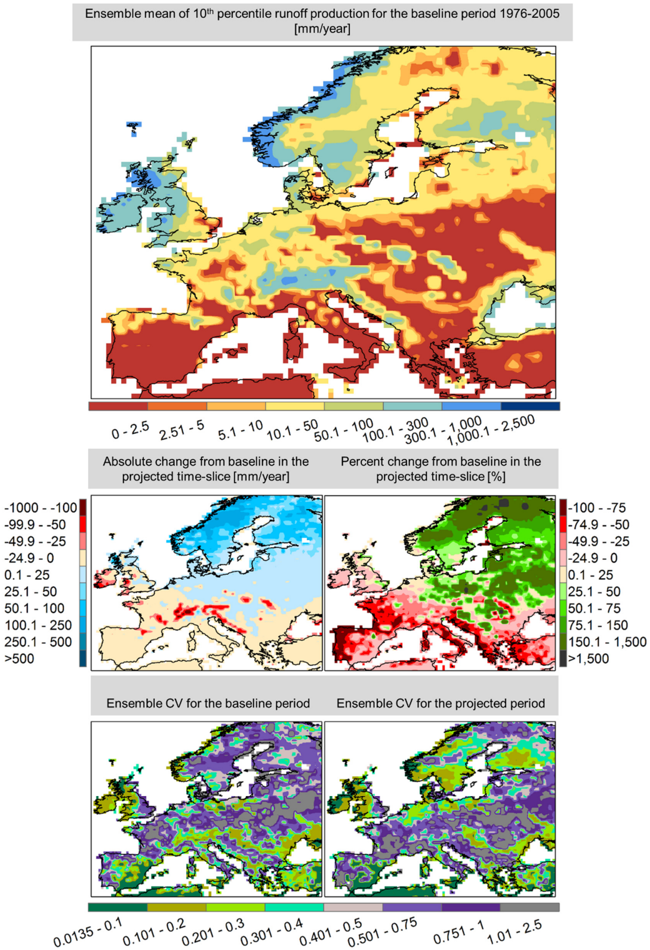

Figure 7. As in Fig. 4, but for bias adjusted Euro-CORDEX data (precipitation and temperature) against WFDEI data.

HESSD
12, 7267–7325, 2015

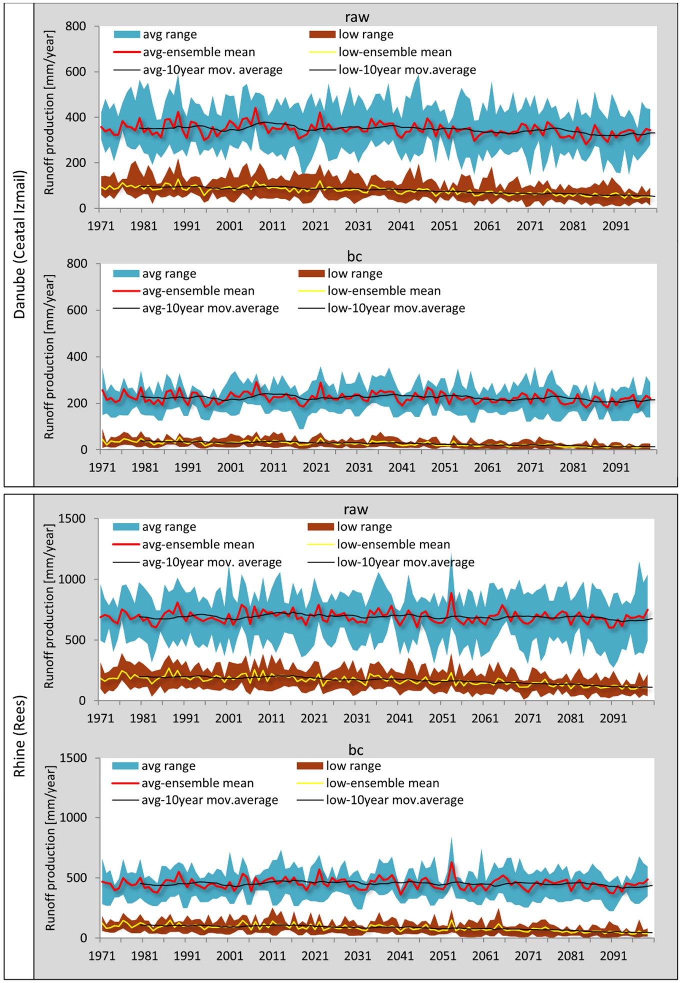

Danube (Ceatal Izmail)
raw
Runoff production [mm/year]
avg range
low range
avg-ensemble mean
low-ensemble mean
avg-10year mov. average
low-10year mov.average
bc
avg-10year mov.average
Rhine (Rees)
1971
1981
1991
2001
2011
2021
2031
2041
2051
2061
2071
2081
2091

Figure 8.

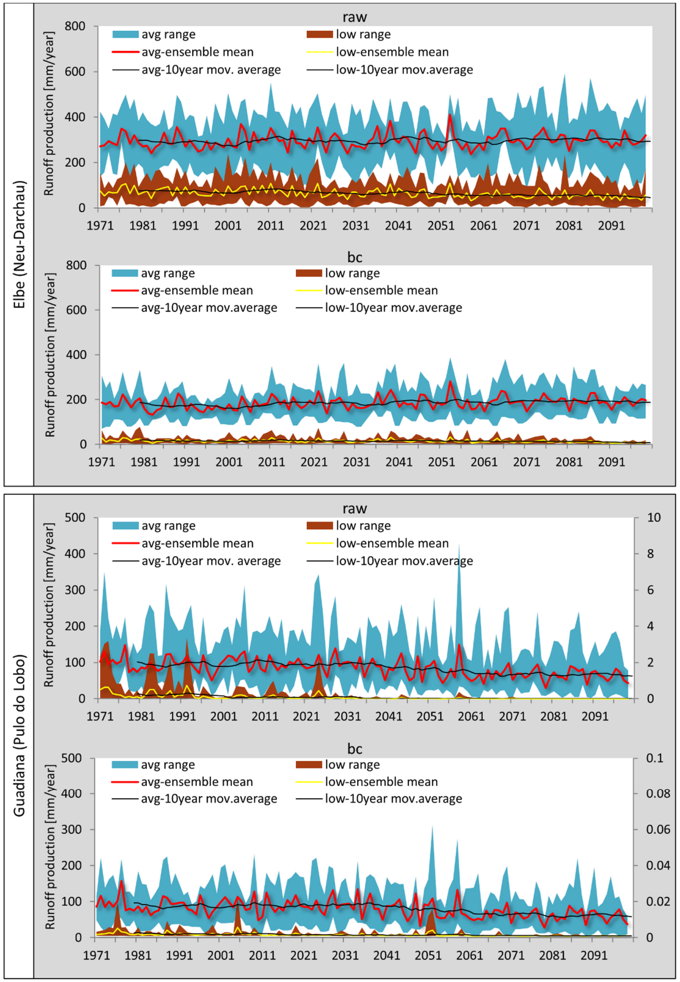

Elbe (Neu-Darchau)
raw
avg range
low range
avg-ensemble mean
low-ensemble mean
avg-10year mov. average
low-10year mov.average
Runoff production [mm/year]
bc
avg-10year mov.average
Guadiana (Pulo do Lobo)
1971 1981 1991 2001 2011 2021 2031 2041 2051 2061 2071 2081 2091

Figure 8.

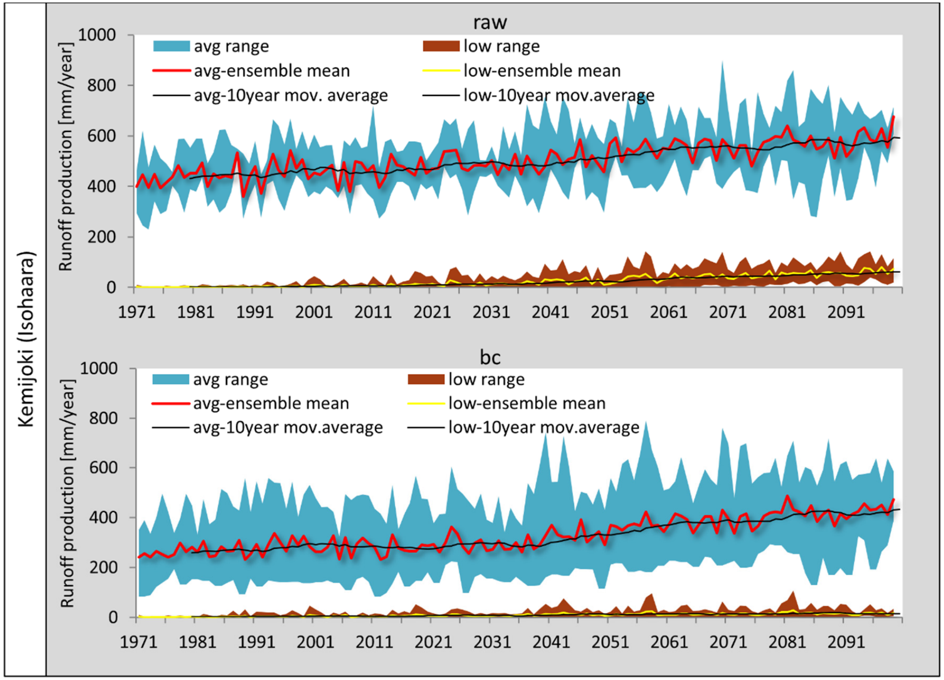

Figure 8. Annual time-series of basin averaged runoff production (average and 10th percentile of annual runoff) for raw and bias adjusted Euro-CORDEX data. For both average and 10th percentile time-series, the ensemble range, mean and 10 year moving average is shown.

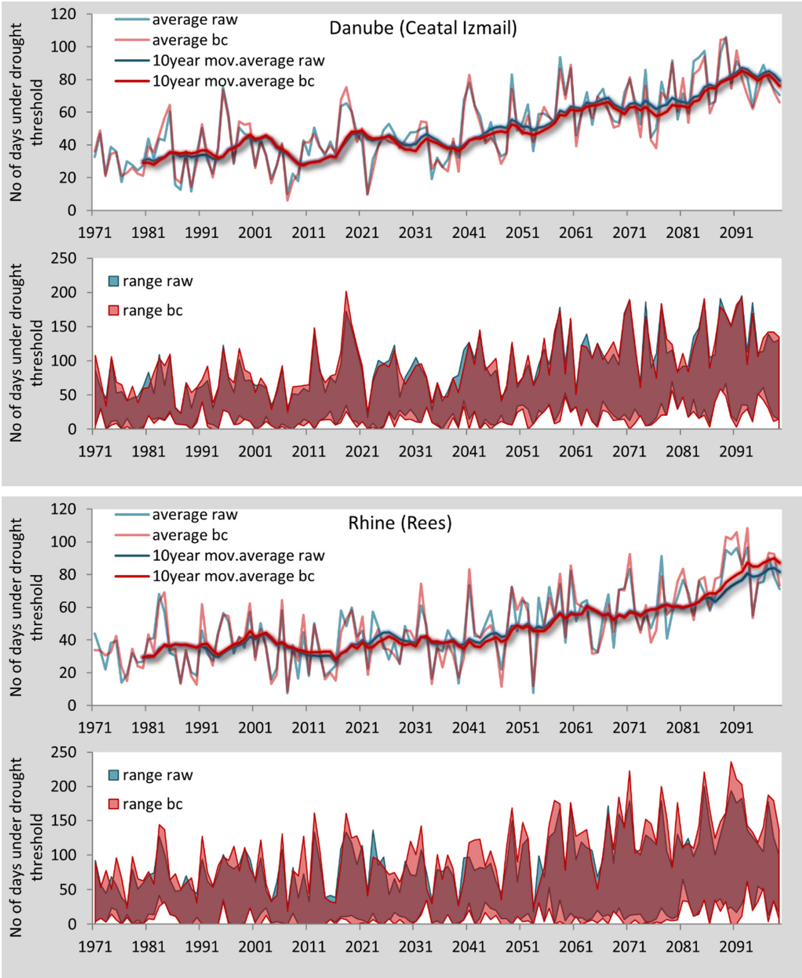

Figure 9.

HESSD
12, 7267–7325, 2015

Title Page
Abstract | Introduction
Conclusions | References
Tables | Figures
Back | Close
Full Screen / Esc
Printer-friendly Version
Interactive Discussion

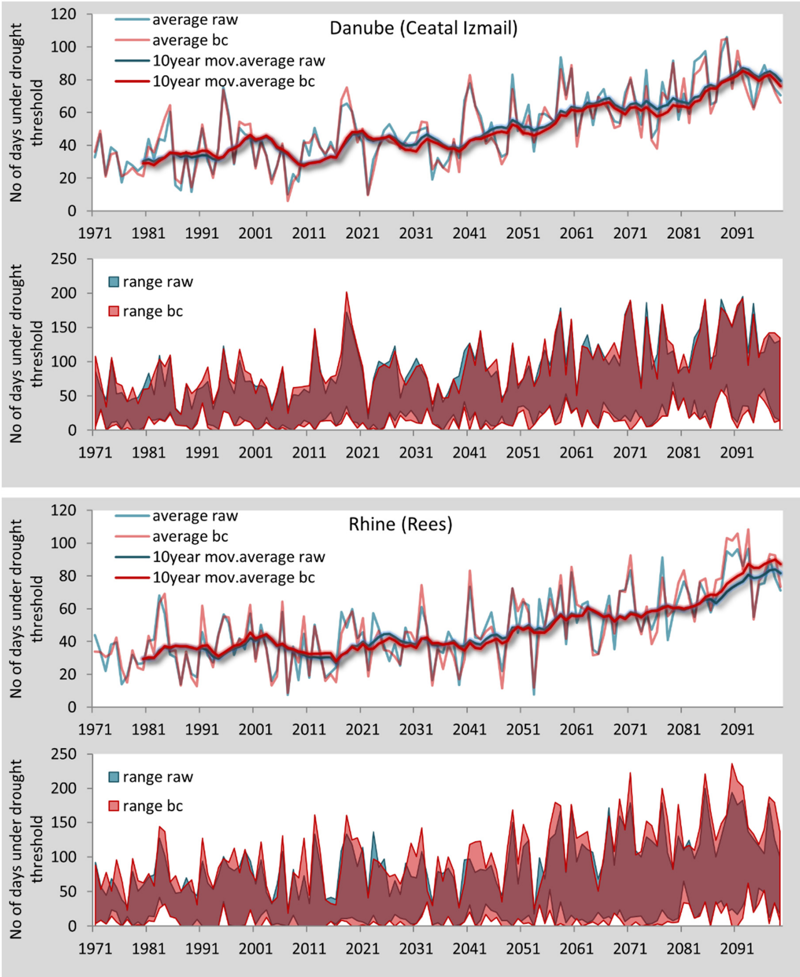

Figure 9.

HESSD
12, 7267–7325, 2015

High-end climate change impact on European water availability and stress

L. V. Papadimitriou et al.

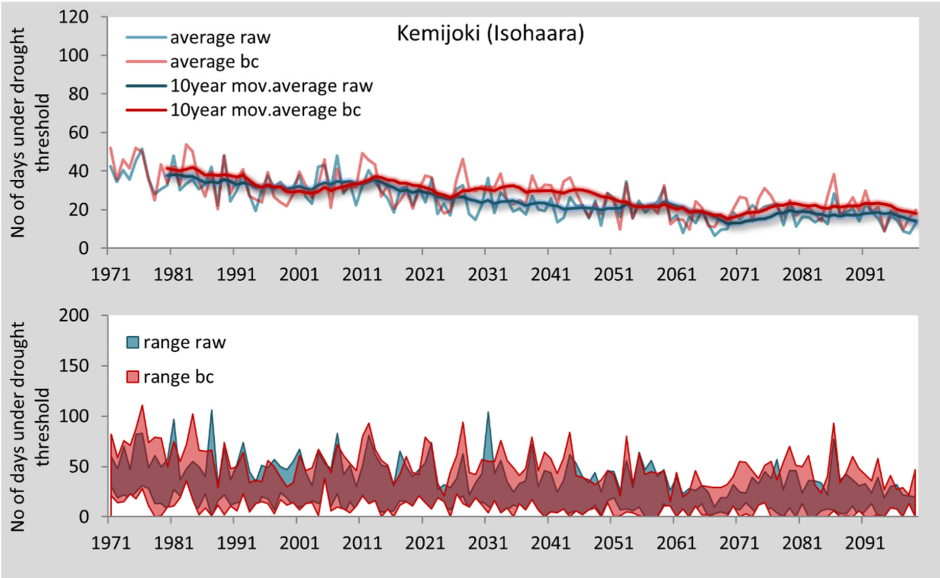

Figure 9. Number of days under drought threshold per year for raw and bias adjusted Euro-CORDEX data. Ensemble mean and 10 year moving average of the ensemble mean (top), ensemble range (bottom).

HESSD
12, 7267–7325, 2015

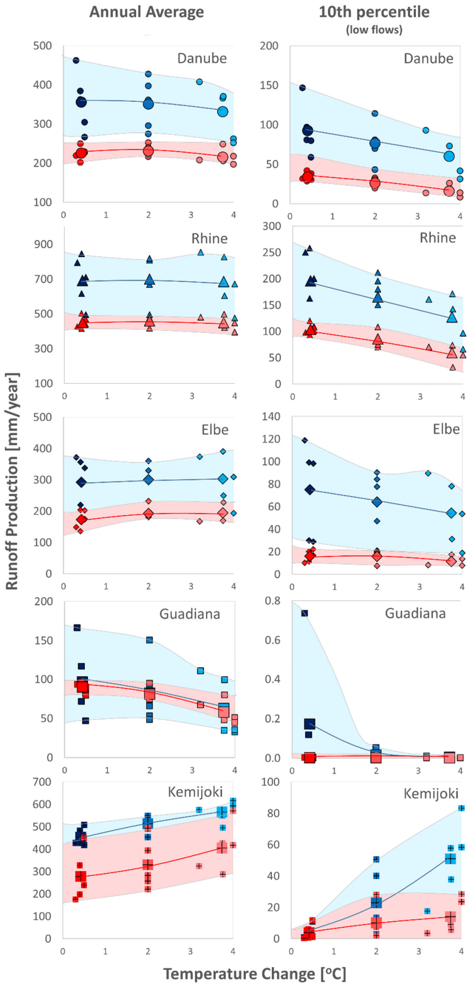

HESSD
12, 7267–7325, 2015

High-end climate change impact on European water availability and stress

L. V. Papadimitriou et al.

Figure 10. Variation of runoff production with respect to temperature change (+2 and +4 SWLs) for raw (light blue) and bias adjusted (light red) Euro-CORDEX data, for both annual average (left column) and 10th percentile (right column) runoff production. Small markers represent the value of each individual model and bigger markers correspond to ensemble mean value.

HESSD
12, 7267–7325, 2015

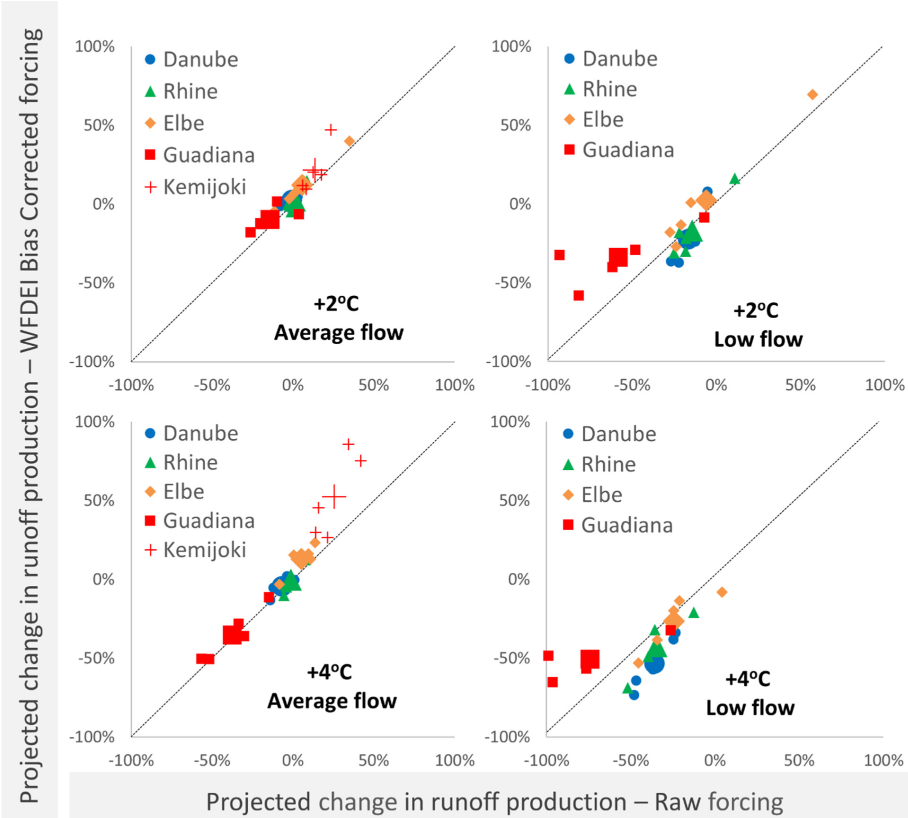

Figure 11. Correlation between projected change in basin averaged runoff production derived from WFDEI-bias adjusted and raw Euro-CORDEX data, for both annual average (left) and 10th percentile (right) runoff production. Correlation is examined at +2 °C SWL (top) and at +4 °C SWL (bottom). Small markers represent the value of each individual model and bigger markers correspond to ensemble mean value.

HESSD
12, 7267–7325, 2015

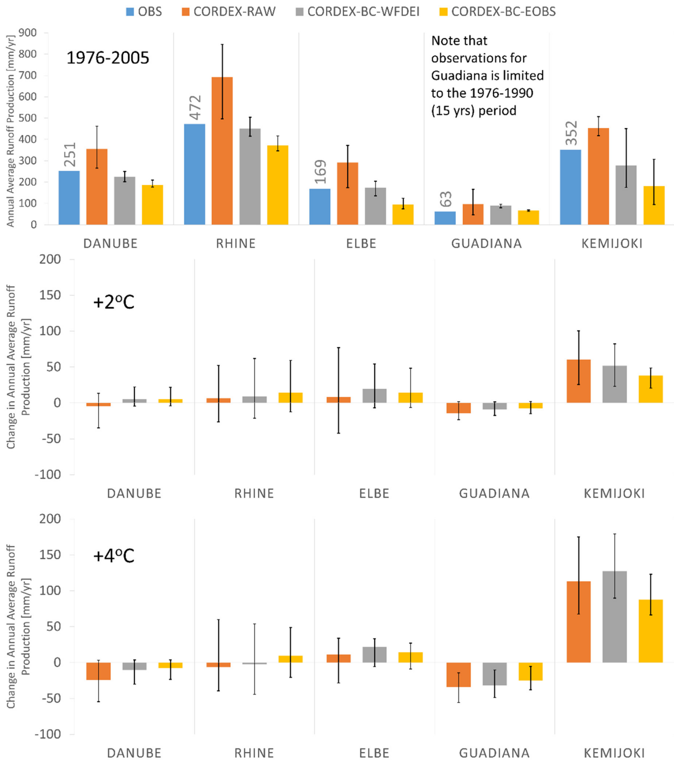

Figure 12. Comparison between the simulations of raw Euro-CORDEX data and bias adjusted against two different datasets (WFDEI and E-OBS) for five study basins. Bars show the ensemble means and error bars the minimum and maximum ensemble member values. (Top row) Annual average runoff production for the period 1976 to 2005. OBS values are derived from GRDC discharge measurements converted to basin averages at the annual time-scale. (Middle row) Percent change in annual average runoff production at the +2 SWL and (bottom row) at the +4 SWL.

HESSD
12, 7267–7325, 2015